HHS Public Access

Author manuscript

Neuron. Author manuscript; available in PMC 2019 March 07.

Published in final edited form as:

Neuron. 2018 March 07; 97(5): 1153–1167.e4. doi:10.1016/j.neuron.2018.01.028.

Signaling mode of the broad-spectrum conserved CO_2 receptor is one of the important determinants of odor valence in *Drosophila*

Dyan MacWilliam[1], **Joel Kowalewski**[2], **Arun Kumar**[1], **Crystal Pontrello**[1], and **Anandasankar Ray**[1,2]

[1]Department of Molecular Cell and Systems Biology, University of California, Riverside, Riverside, CA 92521, USA

[2]Interdepartmental Neuroscience Program, University of California, Riverside, Riverside, CA 92521, USA

SUMMARY

Odor-detection involves hundreds of olfactory receptors from diverse families, making modeling of hedonic valence of an odorant difficult, even in *Drosophila melanogaster* where most receptors have been deorphanised. We demonstrate that a broadly-tuned heteromeric receptor that detects CO_2 (Gr21a, Gr63a) and other odorants is a key determinant of valence along with a few members of the *Odorant* receptor family in a T-maze, but not in a trap assay. Gr21a and Gr63a have atypically high amino acid conservation in Dipteran insects and use both inhibition and activation to convey positive or negative valence for numerous odorants. Inhibitors elicit a robust *Gr63a*-dependent attraction, while activators, strong aversion. The attractiveness of inhibitory odorants increases with increasing background CO_2 levels, providing a mechanism for behavior modulation in odor blends. In mosquitoes, valence is switched and activation of the orthologous receptor conveys attraction. Reverse-chemical-ecology enables identification of inhibitory odorants reduce attraction of mosquitoes to skin.

eTOC

Insects sense a variety of odors using numerous transmembrane receptors and instantaneously like or dislike them. We find that only a few receptors explain instantaneous behavior in a T-maze, including a key conserved receptor that detects several odorants and CO_2.

CORRESPONDING AUTHOR: Anandasankar Ray, Department of Entomology, University of California Riverside, 3401 Watkins Drive, Riverside, CA 92521, USA, Phone: +1(951) 827-5998, Fax:+1(951)827-3086, anand.ray@ucr.edu.

Author Contributions. D.M planned and performed the electrophysiology and behavior experiments and wrote the first draft of the manuscript. J.K planned and performed the computational analyses; A.K performed *Gr63* mutant electrophysiology experiments; C.P assisted with behavior assays; A.R planned the experiments, performed some computation analyses, managed the project, and wrote the final version of the manuscript with help from J.K.

Declaration of Interests. A.R. is founder, shareholder and President of Sensorygen Inc. A.R. and D.M. are listed as inventors on a pending patent application related to this work filed by the University of California Riverside.

INTRODUCTION

In *Drosophila melanogaster*, odorants activate receptors belonging to diverse chemoreceptor gene families expressed in odorant receptor neurons (ORNs) of the antenna and maxillary palp (Croset et al., 2010; Vosshall and Stocker, 2007). The majority of ORNs express members of the olfactory receptor (*Or*) gene family. *Ors* are highly divergent across insect families (Robertson et al., 2003), and their repertoires are tuned to species-specific environments. *Ors* are absent outside of hexapoda (insects) (Eyun et al., 2017) and likely a result of adaptation to flight in insects, long after hexapoda became terrestrial (Missbach et al., 2014). A subset of ORNs express ionotropic receptors (*Irs*). In contrast to *Ors*, *Irs* are highly conserved across insects, and they detect stimuli which are ecologically relevant to most insects such as water, acids, and bases (Croset et al., 2010; Silbering et al., 2011). Antennal *Irs* are more ancient and found in Protostomia like Mollusca and Nematoda (Eyun et al., 2017). Gustatory receptors (*Grs*), are considered the most ancient of the chemosensory receptor proteins in arthropods and have been found in Placozoa genomes (Eyun et al., 2017). While their function has mainly been studied in the taste system in *Drosophila*, two notable exceptions are *Gr63a* and *Gr21a*, which are expressed in the olfactory system and show a strong conservation with their orthologs in other *Dipteran* species, and, most notably, in mosquitoes (Jones et al., 2007; Kwon et al., 2007).

Gr63a and *Gr21a* function together as detectors of CO_2. In flies, activation of the CO_2 receptor neuron (ab1C) leads to a robust avoidance response in a T-maze (Suh et al., 2004). Flies avoid CO_2 even at concentrations that produce only small increases in spike activity, and artificial stimulation of these neurons demonstrates that activation of ab1C alone is sufficient to elicit avoidance (Suh et al., 2007). However, the aversion to CO_2 is context and state-dependent. In a 16-hour wind-tunnel assay or a 20-min walking assay, highly active female *D. melanogaster* (>2.3mm/sec) show increase in numbers near a 5% CO_2 port. This attraction is also dependent on starvation state and circadian rhythm, and is *Gr63a*-independent and *Ir25a*-dependent (Breugel et al., 2017). Conversely, the passive flies in the walking assay still show *Gr63a*-dependent aversion as in the T-maze.

There are also differences across species in the valence of CO_2, with some related *Drosophila* species not avoiding CO_2 in a T-maze despite sensing it (Pham and Ray, 2015; Pan et al. 2017). In more distantly related dipterans like mosquitoes, CO_2 is an attractant important for navigation toward human hosts, and is a synergist that enhances attraction to other host cues (Takken and Knols, 2010). The mosquito CO_2 receptor neuron (cpA) also responds directly to human skin odorants, and silencing cpA impairs navigation to both CO_2 and these other odorants (DeGennaro et al., 2013; Tauxe et al., 2013; Turner et al., 2011).

Early studies describe ab1C and cpA as narrowly tuned to CO_2 (de Bruyne et al., 2001; Suh et al., 2004); more recently, these neurons have been shown to respond to a diversity of odorants (including the aforementioned odorants emitted by human skin) belonging to multiple chemical classes (Lu et al., 2007; Tauxe et al., 2013; Turner et al., 2011). Responses to these CO_2-receptor neuron agonists are largely conserved between flies and mosquitoes, and it has been demonstrated that agonists other than CO_2 can both attract mosquitoes and repel flies (Tauxe et al., 2013). A handful of CO_2 receptor neuron inhibitors have also been

identified (Tauxe et al., 2013; Turner and Ray, 2009; Turner et al., 2011), and behavioral studies show them to decrease the number of mosquito landings on a human hand (Tauxe et al., 2013).

Here we investigate the contribution of the highly conserved *Gr21a/Gr63a* receptor to olfactory behavior in *Diptera*. We start by showing that they play a role in detection of an ecologically important class of odorants, amines, and find that they strongly inhibit the CO_2 receptor neuron in both flies and mosquitoes. Surprisingly, amines and other inhibitors of the CO_2 neuron strongly attract *Drosophila* in a T-maze in a *Gr63a*-dependent manner. We find that the behavioral valence of an odorant is significantly correlated with activity of this single class of neuron. We also find that increasing background levels of CO_2 enhances the attractiveness of inhibitors, and can even switch the valance of an inhibitory odorant from avoidance to attraction, providing a peripheral mechanism to explain enhanced activity of odor blends. An unbiased computational analysis indicates that the CO_2-neuron along with a few broadly-tuned Ors together can predict the behavior in a T-maze for a majority of 54 odorants tested. This computational approach also allows for successful modeling of trap assay data, but interestingly, a different set of Ors rather than the CO_2 neuron receptors predict this longer time-course behavior. Taken together, our results suggest that the *Gr63a*/*Gr21a* receptor neuron pathway may have evolved to function with *Or* pathways to encode both positive and negative hedonic valence across multiple chemical classes in rapid response to odorants. This pathway, however, may be dispensable for longer timescale behaviors as seen in flight and trap assays.

RESULTS

Polyamines attract *Drosophila* by inhibiting the CO_2 receptor neuron

Polyamines such as spermidine are important growth regulators in plants, and along with ethylene, are associated with fruit ripening (Pandey et al., 2000). *Drosophila melanogaster* is strongly attracted to spermidine in a T-maze; however, not all of the receptors mediating this attraction have been identified (Min et al., 2013). Although spermidine activates sub-populations of *Ionotropic receptor (Ir)*-expressing neurons in coeloconic sensilla, inactivation of these neurons did not result in reduced attraction (Min et al., 2013; Silbering et al., 2011). Two related polyamines, cadaverine and putrescine, are detected by *Ir76b+,Ir41a+* ORNs. Although the *Ir76b* mutant shows significant reduction in attraction, there is still residual attraction at ~50% of control (Hussain et al., 2016). We tested the contributions of members of the *Odorant receptor (Or)* gene family using flies lacking the obligate Or co-receptor *orco*, and found that attraction to spermidine in a T-maze was also not affected when *Ors* are inactive (Figure 1A). The remaining class of known olfactory receptor is the CO_2 receptor encoded by members of the *Gustatory receptor* family (*Gr21a* and *Gr63a*). We found that attraction to spermidine was greatly reduced in flies lacking *Gr63a* (Figure 1A).

Odor-mediated behaviors can be complex, and distinct behavioral steps may be mediated by different receptors depending on the context of the stimulus and the internal state of the animal (Bräcker et al., 2013; Lin et al., 2013; Turner and Ray, 2009; Wasserman et al., 2013). Since the T-maze assay tests short-term behavioral response to odor gradients (within one minute), we also tested attraction to spermidine using a second, long-term trap assay.

Surprisingly, in the context of this 24 h assay, we find that attraction is not dependent on *Gr63a* (Figure 1B).

The results of the *Gr63a*-dependent attraction in a T-maze were puzzling, since previous studies have demonstrated that in this assay, activation of the *Gr21a*/*Gr63a* expressing ab1C neurons by CO_2 and other odorants results in a robust avoidance behavior (Jones et al., 2007; Suh et al., 2004; Tauxe et al., 2013; Turner and Ray, 2009). This *Gr63a*-dependent aversion is also seen in a longer-term 30 min assay in which *D. melanogaster* is passive, similar to the T-maze, whereas flies in an active state of motion (>2.3mm/sec) are briefly attracted to CO_2 (Breugel et al., 2017). However, this attraction is *Gr63a*-independent (Breugel et al., 2017) suggesting another explanation. We therefore performed single-sensillum electrophysiology on the ab1 sensilla to measure the response of the ab1C to spermidine. We used *orco* mutant flies where the action potential of the C neuron is clearly quantifiable since the three Or-expressing neurons (A, B and D) are silent. We discovered that spermidine inhibited the baseline activity of ab1C in a dose-dependent manner (Figure 1C), suggesting a model where inhibition of a repellent neuron causes attraction. While inhibitory odorants have been shown to block aversion to CO_2 (Turner and Ray, 2009), we did not anticipate that there would be a dose-dependent attraction, via inhibition alone, of the ab1C neuron's baseline activity.

In order to confirm that attraction to spermidine is dependent upon inhibition of the ab1C neuron, we blocked action potentials in those neurons by driving an inwardly-rectifying potassium channel (Kir) as has been shown earlier for other Gr-expressing neurons (Charlu et al., 2013). Consistent with our previous observation in the *Gr63a*- mutant flies, attraction to spermidine was abolished (Figure 1D). Silencing the ab1C neurons by pre-exposure to a high concentration of 2,3-butanedione (10%), as reported previously (Turner and Ray, 2009), also abolished attraction to spermidine (Figure S1A). The results demonstrate that a polyamine can inhibit the CO_2-receptor neuron, and that inhibition of this avoidance pathway is necessary for attraction towards the odorant in a T-maze. The structurally similar polyamine odorants ethylenediamine and piperazine also inhibited the baseline activity of ab1C, strongly suggesting that similar chemicals show inhibition (Fig. 1E, 1F). The simplest interpretation of these results is that inhibition of an aversive sensory pathway contributes to attraction up a concentration gradient towards the inhibitor (Fig. 1G).

Monoamines also inhibit ab1C and cause attraction

Like the polyamines, monoamines are also known to elicit attraction in *Drosophila*; however, in contrast to spermidine, this attraction was shown to be largely dependent on the Ir92a receptor (Min et al., 2013) (Figure S1B). We were curious whether these odorants might also inhibit the ab1C neuron, and whether this inhibition contributes to attraction in a T-maze. From a panel of primary, secondary, tertiary and cyclic monoamines, every compound tested strongly inhibited ab1C activity in a dose-dependent manner (Figure 2A). We then tested butylamine, dimethylamine and trimethylamine, behaviorally in *Gr63a* mutants. As with spermidine, wild-type flies were attracted to these monoamines, and this attraction was reduced in flies lacking *Gr63a* (Figure 2B). This suggests that in addition to the *Ir92a* pathway, the *Gr63a*/*Gr21a* pathway is also required for attraction to amines in a T-maze. The

simplest interpretation is that attraction to monoamines in a T-maze requires both activation of the *Ir92a* pathway, and a concomitant inhibition of the *Gr63a/21a* pathway.

Inhibition of the CO_2 receptor neuron by amines is conserved in mosquitoes

The *Drosophila* CO_2-receptor proteins (Gr21a and Gr63a) are well conserved in several insect species, including mosquitoes, where their homologs (Gr1, Gr2, and Gr3) are expressed in the CO_2-sensitive cpA neurons of the maxillary palps. In mosquitoes, however, the behavioral valence is switched, and activation of the cpA neurons by CO_2 and other odorants causes attraction (Takken and Knols, 2010; Tauxe et al., 2013; Turner et al., 2011). ORN response to odorants that are ligands of the Gr21a/Gr63a receptor is conserved in mosquitoes, and we have demonstrated that detection of skin odorants by the cpA neuron also plays a central role in host-seeking behavior (Tauxe et al., 2013; Turner et al., 2011). There is little understanding as to how mosquitoes and other blood-seeking insects detect polyamines and monoamines, which are present in human emanations (Bernier et al., 2000; Braks and Takken, 1999; Ellin et al., 1974; Geier et al., 1999; Krotoszynski et al., 1977; Taneja and Guerin, 1997). Electrophysiological responses to amines have been detected in grooved peg sensilla located on the mosquito antenna and in sensilla of the labellum (Davis and Sokolove, 1976; Kwon et al., 2006; Meijerink et al., 2001; Qiu et al., 2006), but the identity of receptors responsible for such detection remains unknown. Based on the sequence conservation of CO_2 receptors, we predicted that cpA neurons would also detect amines. We therefore expanded our study to include the *Aedes aegypti* mosquito, a vector of the dengue and yellow fever viruses.

Using single-sensillum recordings from the *A. aegypti* cpA neurons, we found that polyamines and monoamines also inhibited the *A. aegypti* cpA neuron. Spermidine and the closely related spermine strongly inhibit baseline cpA activity at concentrations similar to those effective in *Drosophila* (Figure 3A,B). A panel of monoamines also inhibited cpA activity strongly (Figure 3C, D). Since many of these inhibitors may be present in the human environment along with activators such as CO_2 and skin-odorants, we were curious to look at the effect of mixtures on cpA. Spermidine acts only as a weak inhibitor when overlaid on CO_2 (Figure 3D, E). In contrast, monoamines were effective in their ability to inhibit cpA activation by CO_2. (Figure 3D), suggesting that these may prove to be useful CO_2 masking agents in control applications.

Spermidine can mask attraction towards human skin odors

While spermidine can effectively inhibit room air activation (Figures A, E) and baseline activity (Figure 3F) of the cpA neuron, we found that it does not inhibit cpA activation by CO_2, even at very high concentrations, either when it is overlaid on a pulse of CO_2 (Figure 3D, F), or when CO_2 is delivered onto a prolonged pulse of spermidine (Figure 3F). In contrast, even low concentrations of spermidine (0.1%) inhibited the activation of another strong cpA activator, cyclopentanone (Figure 3G). Since cpA plays a role in detection of some human skin odorants that are similar in structure to cyclopentanone (Tauxe et al., 2013), we expect that an inhibitor such as spermidine might reduce cpA detection of human odorants. Indeed, the attraction of female *A. aegypti* mosquitoes to human skin odorant was significantly lowered in the presence of spermidine in a 2-choice assay (Figure 3H, I).

Mutant *A. aegypti* mosquitoes lacking the *Or* co-receptor *orco* still avoided the spermidine-treated side, demonstrating that avoidance was not due to detection via *Or* receptors, consistent with the notion that avoidance is due at least in some degree to inhibition of the *Gr*-dependent cpA neuron (Figure 3J). However, when spermidine was presented along with a complex attractive cue such as a human arm, which emits warmth and moisture in addition to skin odorants, masking was overcome (Figure S2A, B).

Odor valence is modulated by the balance of ab1C activators and inhibitors

In natural surroundings, an insect is likely to encounter mixtures containing both activators and inhibitors of the Gr21a/Gr63a neuron. Moreover, the concentrations of these odorants may vary widely in different environmental contexts. For example, background levels of CO_2 vary in a diel rhythm due to changes in carbon fixation by plants or due to changes in the proximity of respiring plants or animals, and levels of CO_2 emitted by fruit can also vary with stage of ripeness (Faucher et al., 2006). In order to systematically investigate the effect of CO_2 concentration on valence of an inhibitory odorant, we performed experiments with a strong inhibitor, ethyl pyruvate (Tauxe et al., 2013). Analyses of behavior across several concentrations correlate well with degree of inhibition of the ab1C neuron, except at the highest concentration tested (1%) (Figure 4A,B). Aversion to the 1% ethyl pyruvate concentration is likely to be *Or*-mediated, since *orco*− flies are attracted to it (Figure 4B). Predictably, attraction to ethyl pyruvate is dependent upon *Gr63a*; however, the *Or*-mediated response is not itself sufficient to elicit aversion.

We examined the effects of an elevated background of CO_2 on the valence of the aversive concentration of ethyl pyruvate in wildtype flies. Although 1% ethyl pyruvate was avoided in ambient levels of CO_2, valence was reversed, becoming more attractive with increasing concentrations of background CO_2 (Figure 4C,D). These results indicate that the valence of an ab1C inhibitor in a T-maze is context-dependent, and influenced by how components in a mixture affect the relative balance of the *Gr21a/63a* and *Or/Ir* inputs.

CO_2 receptor neuron activity is an important predictor of behavioral valence

The activity of the ab1C neuron is affected by diverse odorants such as amines and CO_2, as well as several other classes of odorants (Tauxe et al., 2013; Turner et al., 2011). We tested a panel of 14 structurally diverse odorants including some of the known activators and inhibitors and a few additional compounds previously known to be behaviorally-active (Knaden et al., 2012; Keene et al., 2004) for behavior in a T-maze (Figure 5A). Flies predictably avoided ab1C activators, and were attracted to ab1C inhibitors. Half the compounds showed significantly reduced avoidance and attraction in flies lacking *Gr63a* (Figure 5A).

Our results suggest an intriguing possibility that the highly conserved Gr21a/Gr63a+ neuron may determine the valence in a T-maze of many ecologically important odorants, spanning multiple chemical classes. In order to test this further, we selected a large panel of 60 structurally-diverse odorants, of which 54 were randomly selected from a larger panel that have been tested for activity on 24 Or receptors, the majority of those present in the antenna (Hallem and Carlson, 2006). We systematically tested this diverse panel of odorants in a

quantitative T-maze assay using wildtype *Drosophila*. Since these odorants are also detected by Or family receptors, it begs the question as to how the Ors contribute to valence. A previous study found that the responses of these 24 antennal Ors to a large panel of odorants could not predict the behavioral valence observed in a 24 hr trap assay (Knaden et al., 2012). Since our behavioral data is from a T-maze assay which measures immediate olfactory responses over 1 min, we were curious whether the 24 Or responses could explain the odor valence we observed. Using Principle Component Analysis of the 24-dimensional receptor response-space, we found that the first principle component represents 41% of the variance in electrophysiology response (Figure 5B). When we tested the correlation between the first principle component and the T-maze preference index for the odorants, we uncovered a weak negative correlation (r= −0.295) (Figure 5C). Taken together, these results suggest that receptors other than from the Or-family are also likely to have significant contributions to the odorant valence.

Interestingly, when we systematically tested the 60 odor panel in the T-maze assay using *orco* co-receptor mutant flies that lack activity of all Or receptors, nearly 72% of the odorants elicited attraction or avoidance within a minute in wildtype flies, and a small fraction (16%) lost behavioral responses in the *orco* mutant (Figure 5D). A few of the Orco-dependent odorants are structurally related (5–6 carbon alcohols), suggesting that their behavior may depend on only a few *Or* receptors. Surprisingly, *orco* mutants became attracted to 10% of odorants that they usually avoid, suggesting that the Ors detecting these odorants likely mediate avoidance in a T-maze, and in their absence, there are other receptors that likely cause attraction (Figure 5D). These results are consistent with our model that the *Gr21a/Gr63a*+ neuron may contribute to behavioral valence of a large number of odorants in the T-maze assay. This finding is different from the larval stage of *Drosophila* where the behavioral responses for most odorants are *Orco*-dependent Fishilevich et al., 2005), and activity of the Ors can predict behavioral valence successfully (Kreher et al., 2008).

In order to test whether the behavioral response could be mediated by the *Gr21a/Gr63a+* neuron, we used single unit electrophysiology to test the activity of the behaviorally tested odorants. As done previously, we recorded from the *orco*− flies to enable counting of the ab1C neuron's activity, which is obscured in wild-type flies by the larger spike amplitudes from the ab1A and ab1B cells (Turner and Ray, 2009). Many odorants from this panel showed activation or inhibition of the ab1C neuron (Figure 6A). Responses were lost in the ab1 sensilla of *Gr63a*$^{-}$,*orco*$^{-}$ flies, indicating that they likely act through the CO_2-receptor (Table S1). Plotting the ab1C activity alongside the T-maze behavior index revealed a clear trend, showing that most activators are aversive, and inhibitors are attractive (Figure 6A). The few non-ab1C repellents are structurally related acids, previously shown to be ligands of *Ir64a/Ir8a* (Benton et al., 2009; Silbering et al., 2011; Yao et al., 2005). We find that activity of the *Gr21a/Gr63a+* neurons is a good predictor of compound valence in wildtype flies (R=0.5835, pval=<0.00001), and prediction is further improved in *orco*$^{-}$ flies (R=0.8314, pval=<0.00001) (Figure 6B, C).

Gustatory receptors (*Grs*), are considerably more ancient as chemosensory receptors in arthropods than the *Or* and *Ir* families (Eyun et al., 2017). Amongst Dipteran species, we

plotted the evolutionary rate of all known and anticipated olfactory receptors from the 3 receptor families (Or, Ir, Gr) obtained from the OrthoDB database (http://orthodb.org) and found lower rates of evolution for the Gr21a and Gr63a receptor proteins in comparison to all other odor-detecting receptors known, with the exception of the co-receptors Orco and Ir25a (Figure 6D, top). Conversely, the percentage identity of amino acids between the *D. melanogaster* proteins and their closest homologs in two mosquito genomes also shows that Gr21a and Gr63a are far better conserved than the other receptors, matched only by the co-receptors (Figure 6D, bottom).

Our previous experiments with ethyl pyruvate had shown that the inhibitory attraction mediated by the Gr21a/Gr63a-neuron could override strong aversion mediated by the Or/Ir family receptors. In complimentary experiments, we directly tested the repellency conveyed by the CO_2-receptor versus the Or-family receptors and found that CO_2 aversion overrides Or-mediated repellents that are known from the literature, geosmin and benzaldehyde (Figure S2C). Taken together, these results indicate that for behaviorally-active odorants tested in this study, activation or inhibition of the highly conserved Gr21a/Gr63a-receptor neuron acts as one of the key determinants of hedonic valence in the short time-course T-maze assay (Figure 6E).

Predicting behavior with and without ab1C activity

In order to take an unbiased approach to assess the behavioral contribution of the 24 ORs and the Gr21a/Gr63a-expressing (ab1C) neurons activity, we performed a series of statistical and feature-selection approaches to identify receptor(s) that can optimally predict behavior (Figure 7A). Regression analysis of T-maze Preference Index (PI) of the 54 odorants on the known activities of the 24 ORs was not statistically significant ($p > .05$). However, adding activity of the ab1C neuron, the model could explain 63% of the variation in behavior ($p = 0.03$). Interestingly, the activity of ab1C alone was also statistically significant ($p<0.001$) and favored according to a measure of model fit (BIC = 24.6) (Figure 7B,C).

We next identified the minimum number of receptors that could predict behavior, as was done previously for larval behavior (Kreher et al., 2008). The 25-predictor model (24 Ors and ab1C) was analyzed using stepwise regression, entailing the sequential removal of predictors until converging upon an optimal subset. Candidate models were screened using values of R squared, Mallow's Cp and the Bayesian Information Criterion (BIC). Surprisingly, only a two-predictor model with ab1C and Or85f was retained when using the stepwise selection method alone as before (Kreher et al., 2008). In order to further control if this model was a byproduct of a few influential odorants affecting the regression fit or spurious correlations with the PI, the odor space was sampled from with replacement, resulting in thousands of random combinations of 54 odorants. Running the stepwise regression iteratively on 5000 resamples and recording the selection rate for each predictor in the final model suggested that a model including ab1C, Or2a, Or67a, Or59b, and Or19a would generalize well across many odorants. High selection rate was for the most part consistent with the t statistic assigned to each predictor when fitting the full model to all 54 odors (Figure 7B). A least squares regression model with these predictors when fit on the original data resulted in the linear equation, Avg. PI = −0.23 − 0.09 *Or*67a + 0.02 *Or*2a

− 0.04 *Or*59b − 0.03 *Or*19a − 0.14 ab1C (Figure 7E). Most selected predictors are broadly tuned ((Hallem and Carlson, 2006), DoOr database (http://neuro.uni-konstanz.de/DoOR/default.html)), consistent with the expectation that they should remain informative across many different odor samples. The selection rate for ab1C was the highest of all 25 and further emphasized its role in predictions of odor valence (Figure 7D). After identifying the potentially optimal predictors, we evaluated performance of the 5-predictor model and compared it to ab1C alone, or ab1C and a broadly tuned Or such as Or67a, which is also consistently picked up across several selection methods. It was evident that smaller models ultimately provided better or similar predictions across 5000 resampled odor sets (Figure 7G). Given further evidence that ab1C activity was more informative than Ors even after controlling for overfitting, we revisited the comparison between ab1C and the 24-Or model (Figure 7B) but using 1000 folds (10-fold cross-validation repeated 100 times), opting for regularized regression to improve performance of the larger 24-Or model. The averaged performance metrics showed ab1C explained 41% of the variability in behavior across the 1000 resamples, as compared to 22% for the all Or model (Figure 7F).

It remained unclear from these analyses, however, to what extent odor valence was indeed a linear function of receptor/neuron activity in the antenna and if this was an unreasonable constraint. Recent studies have suggested the possibility of non-linear interactions in contribution of ORNs or glomerular activities to behavior (Badel et al., 2016; Bell and Wilson, 2016). We therefore broadened the scope of our analysis using different machine learning algorithms that are more flexible and conducive to capturing non-linear relationships. Using these, we tried to determine (1) at what frequency would ab1C meaningfully improve predictions regardless of the algorithm being used, (2) what are the consensus optimal predictor sets selected across these algorithms, and (3) which algorithms minimize prediction error after removing uninformative predictors (supplemental methods). To compare the differing approaches and models, error rates were evaluated using bootstrap validation (1000 resamples) or 10-fold cross-validation, repeated 100 times (1000 folds). These techniques involved training each algorithm on a matrix of receptor activities to odorants, subsequently predicting the preference index for samples or odorants that were not used during the training. Across algorithms for identifying optimal predictors, ab1C was always ranked above the 24 Ors, followed by Or67a and Or22a. Intriguingly, Or22a, which displays a more complex relationship with behavior was high on every list but was nevertheless missed by the previous OLS regression and stepwise removal (Figure S3B; Figure S4C). In general, models sensitive to non-linearity and interactions amongst the predictors resulted in slight improvement during validation, yet the major determinant was whether ab1C was in the model. Despite implementing many complex algorithms, any improvement approximated our control case, fitting a simple regression model with ab1C and Or67a ($R^2 = 0.45$) (Figure S4A & B). Larger odor samples will undoubtedly favor these sophisticated algorithms, but it remains surprising that ab1C was selected as one of the top predictors of valence for the T-maze behavior generated in this study.

It would be important to ask whether ab1C activity is also a significant predictor for other types of olfactory behavior in longer-term assays such as the wind-tunnel, walking assays, or traps. While large odor sets have not yet been tested in the wind-tunnel, we were able to utilize a large behavioral preference data set generated using trap assays, which had

substantial overlap with the odorants (47/110) that we tested in the T-maze (Knaden et al., 2012). Interestingly, the behavioral preferences across the 2 assays differ (r = 0.01 p = 0.9; rank ordered correlation for the bottom ten compounds in the T-maze assay rho = 0.44, p = 0.2), and could potentially be occurring through different olfactory pathways. Using a similar approach we were able to identify the top 7 optimal descriptors (Figure S5B). However, unlike with the T-maze, few predictors were individually informative; it was no longer evident that a simple rank ordering from the selection rate was useful. Instead, combinations of the top 7 predictors were reassessed using repeated 10-fold cross-validation, retaining the best performing model. The least squares fit for the winning model resulted in the linear equation, Avg. AI = 0.19511 + 0.07894 Or59b − 0.09033 Or49b − 0.05763 Or98a on the original data (Figure S5D, E, F). These results suggest that the statistical approach we developed can identify odorant receptors that can predict the trap behavior (R^2=0.4), as was possible with T-maze. A more general approach excluding cross-validation and considering activities of all 24 Ors was not sufficient to predict behavior (Knaden et al., 2012). Surprisingly however, ab1C was not a significant predictor of the trap behavior, suggesting that the behavioral responses to these two olfactory assays are likely generated in a fundamentally different manner, using different receptors.

DISCUSSION

Insects use their sophisticated olfactory systems to locate food, host sources and oviposition sites, and to seek out mates. For *Drosophila*, the important sources of volatile cues are in ripened fruit, and for female blood-seeking mosquitoes, attractive cues are found on human skin, in exhaled breath, and other odorous emissions. Investigations into neural pathways dedicated to the coding of ecologically relevant cues has led to progress in the understanding of attraction and avoidance pathways. Behavioral phenotypes have been observed for several narrowly tuned receptors (Ai et al., 2010; Kurtovic et al., 2007; Semmelhack and Wang, 2009; Stensmyr et al., 2012), but for broadly detected food odorants, functional redundancy across multiple *Or*s has confounded analysis (Elmore et al., 2003; Keller and Vosshall, 2007; Semmelhack and Wang, 2009). We find that the single heteromeric receptor encoded by the *Gr* family members *Gr21a/Gr63a* appears to contribute significantly to the encoding of valence for a number of odorant classes in *D. melanogaster*, and uses both activation (aversion) as well as inhibition (attraction) to encode information (Figure 7B). Immediate T-maze behavior mediated via the *Gr21a/Gr63a* neurons appears to override Or-family mediated behaviors in terms of both aversion and attraction (Figure S2C and Figure 4B).

Of particular interest is the attraction generated by inhibition of a receptor. We show that the CO_2 neuron is inhibited by polyamines, some of which are found in fruit (Kakkar, 1993; Kiss et al., 2006; Ough et al., 1981). Polyamines are abundant in all the tissues of plants and animals, and in fruit are important growth regulators associated with ripening (Pandey et al., 2000). Levels of spermidine, spermine, and their structurally similar polyamine precursor, putrescine, vary across plant species, fruit tissues, and stage of fruit development (Kakkar, 1993; Malik and Singh, 2004). Levels of polyamines increase following exposure to environmental stressors, such as chilling (McDonald and Kushad, 1986) and mechanical impact that results in bruising (Valero et al., 1998). Amines are also emitted as metabolic by-products, during the breakdown of organic matter by microorganisms that can influence

palatability and fly oviposition behavior (Stensmyr et al., 2012). In the future, it will be interesting to investigate differences in volatile composition, especially in the context of the important roles inhibitors of olfactory receptors may play, surrounding various microdomains of the fruit established by environmental factors or colonization by different microorganisms.

The *Drosophila* ab1C neuron has a *Gr21a/Gr63a*-dependent average baseline firing rate of ~10–15 spikes/s^{-1} in a CO_2-free airstream (de Bruyne et al., 2001; Faucher et al., 2013; Jones et al., 2007; Kwon et al., 2007). Spontaneous activity occurs in most ORNs, and although many inhibitory odorants have been identified for other olfactory receptors, the behavioral effects of inhibition are not known. In light of recent findings which have indicated the importance of inhibition in the mediation of innate attraction at the level of the lateral horn (Strutz, 2015), this investigation into the role of inhibition at the level of the periphery is extremely important. ORNs connect to specific projection neurons (PNs), and PN's also exhibit a baseline activity which is dependent on input from the ORNs (Kazama and Wilson, 2009). Dose-dependent inhibition of ab1C could therefore also inhibit the second order PNs, and affect activity of a vast connected circuitry leading to behavior. Also, since glomeruli are connected via lateral excitatory and inhibitory connections, odor-mediated inhibition of this pathway could modulate additional antennal glomeruli as well (Olsen and Wilson, 2008; Yaksi and Wilson, 2010).

While the receptors and their ligands are conserved in mosquitoes, the valence conveyed by the orthologous Gr1, Gr2, Gr3- expressing cpA neuron is reversed, such that activation causes attraction. In contrast, we find that spermidine can mask attraction to a skin odor net. This masking effect is likely due to its strong inhibition of the cpA neuron, which also detects skin odorants. However, spermidine is not an effective masker in the presence of a human arm that carries with it additional attractive cues such as heat and humidity. Nevertheless, the effective masking of skin odorant detection by spermidine suggests that it may be a useful component in a blend to make humans less attractive, especially given that both spermine and spermidine are easily available, and already used in some skin creams. Interestingly, some inhibitory compounds that we identified are also present in the human environment, where they are associated with skin extracts, incubated sweat, and urine, suggesting a need to further understand their contribution in attracting mosquitoes to human hosts.

Interestingly, we found that attraction to the ab1C inhibitor spermidine was not dependent on *Gr63a* in *Drosophila* in the long-term trap assay. This suggests that different receptors may contribute to different types of olfactory behavior. A trap assay runs over several hours and likely involves odor detection in a more complex way, as components of behaviors such as oriented flight, landing, arrestation, congregation etc. In a 1-min T-maze assay, the behavioral choice is immediate and likely dependent upon the flies' ability to rapidly orient to olfactory cues. In this regard, the V glomerulus is unusual, and differs from most *Or* glomeruli in that it receives projections from only ipsilateral receptor neurons (Couto et al., 2005; Stocker et al., 1990). While asymmetric neurotransmitter release from bilaterally projecting ORNs has been shown to contribute to odor lateralization (Gaudry et al., 2013), the ipsilateral projecting ab1C neurons may also play an important role in the rapid

directional orientation of flies to odor cues. The Gr and Ir families are ancient, while the Or family is more recent and species specific. While the Gr21a/Gr63a activity is predictive of behavioral valence, and the *orco* mutant remains behaviorally active for many odorants, some behavior cannot be explained by Gr21a/Gr63a and is likely mediated by *Ors* or *Irs*. Many acids, for example, likely act via the Ir pathway. Our results also suggest that behavioral responses to some ab1C ligands can be modified by concomitant detection via *Or* pathways, which likely depends on concentration. It is known that the valence of an attractive odorant can be reversed at higher concentrations via the recruitment of additional repellent Or-glomeruli (Semmelhack and Wang, 2009). Furthermore, when complex odor blends are present, the interaction between the different pathways becomes more complex. Physiological state such as starvation also increases the attractiveness of flies toward food odorants through sNPF increasing presynaptic signaling via sNPF receptors, primarily in the Or42b neurons (Root et al., 2011). These presynaptic gain mechanisms are controlled by action of GABA on $GABA_B$ receptors on Or-expressing ORN terminals to increase the signal, but not in the ab1C neurons (Root et al,. 2008). Here we show that valence of an aversive odorant that inhibits the ab1C neuron can also be modulated, and act as an attractant, simply by increase in the concentration of background CO_2, which likely shifts the relative balance of *Gr* to *Or/Ir* inputs (Figure 6D). These effects are extremely pertinent since the CO_2 receptor neuron is both activated and inhibited by ecologically relevant cues belonging to multiple chemical classes, including ketones, amines, acids and alcohols (Tauxe et al., 2013; Turner et al., 2011, this study).

Amine and poly-amine detecting *Ir* receptors such as *Ir92a* have been identified in *Drosophila* and are expressed in the antenna (Benton et al., 2009; Silbering et al., 2011; Yao et al., 2005), and in the case of *Ir76b*, also in the labellum (Hussain et al., 2016). In mosquitoes, amine-sensitive neurons have been identified in sensilla located on both the antenna and labellum, which are also suspected to express *Irs* (Davis and Sokolove, 1976; Kwon et al., 2006; Meijerink et al., 2001; Qiu et al., 2006). Our analyses suggest the possibility that some *Ir* pathways could act alongside *Gr21a/Gr63a*. We show that both *Gr63a* mutants and *Ir92a* RNAi knockdown flies lose attraction to monoamines, suggesting that the concomitant effect on both pathways is required for the short-term behavioral response observed in a T-maze. This potential coordination between two receptor pathways is also consistent with our observations that *orco* mutant flies, that have both *Ir* and the *Gr21a/Gr63a* pathways intact, show extremely high correlation (r=0.815) between behavior output and ab1C activity for several odorants. It is intriguing to speculate that while the broadly tuned CO_2-sensing receptors are required for valence determination, specificity is achieved through the concurrent activity of the more narrowly tuned *Ir* receptors and circuitry. In the future, uncovering the relationship between the *Gr21a/Gr63a* and *Ir* pathways in the central olfactory system should help to clarify how integration occurs.

An exhaustive statistical analysis to test whether a few selected ORN types could model the T-maze behavior in response to the tested odorants led to a linear model with 4 broadly-tuned Ors (Or2a, Or19a, Or59b and Or67a) and Gr21a/Gr63a. In fact, in every possible unbiased analysis we tried, both linear and based on machine learning (altogether ~20 different methods), the activity of ab1C was consistently selected as the top performing descriptor for behavior predictions. The valence of several odorants therefore depends upon

the *Gr21a/63a* pathway. However, narrowly tuned *Ors* detect odorants that elicit specialized behaviors such as oviposition, or act as pheromones, some that are species-specific (Knaden and Hansson, 2014). Our experiments also illustrate that the valence of ~16% of the odorants are lost and ~10% are altered in the *orco* mutant flies, suggesting the importance of the *Or* pathway. This is consistent with recent studies showing segregation of spatial inputs for attractive and aversive odorants in the Lateral Horn brain region of the second order projection neurons connected to *Or*-neurons (Strutz et al., 2014).

Our receptor-selection approach was also applied to the data for a trap assay, which is fundamentally different in design from the T-maze and in observed behavioral valence of overlapping odors (Knaden et al., 2012). A small subset of receptors were selected to best describe the behavior; however, ab1C was not selected. This suggested that long term navigation behavior to odorants in the trap assay is somehow different than in the T-maze assay that measures responses in 1 minute and does not depend on the activity of the ab1C. The trap assay occurs over several hours and is similar to the wind-tunnel assay in timescale, suggesting that long-term navigation or arrestation at an odor source could be dictated by different receptors and circuits than those needed for rapid response as in a T-maze. It is important to note that these assays are artificial situations created in the lab and likely reflect only small parts of olfactory navigation behavior in the wild, where a fly is likely to encounter odorants in several complex contexts including slow changes (gradients) or rapid changes (plumes or landing). It is conceivable that the T-maze behavior represents one type of rapid change that requires an instantaneous response to an odorant. In this regard, we note with interest that second order projection neurons connecting to the ab1C-specific V glomerulus in the antennal lobe show a unusually high level of diversity amongst PNs (Bräcker et al., 2013; Lin et al., 2013). Axons of the PNs from the V glomerulus innervate numerous higher brain structures such as the lateral horn and mushroom body calyx, as well as multiple other regions of the protocerebrum, such as the superior dorsofrontal protocerebrum, inner dorsolateral protocerebrum, superpeduncular protocerebrum, and caudal ventrolateral protocerebrum. It is possible that the ab1C and other *Or/Ir* pathways interact at this higher level. We also note with interest that the Gr63a mutant is defective in responding to a few compounds that do not activate or inhibit it. Interestingly, co-activation of the CO_2-detection pathway in mosquitoes can dramatically increase behavioral attraction to skin odorants (Dekker et al., 2005; Webster et al., 2015), as well as to warm objects or visual stimuli like a dark object (McMeniman et al., 2014; van Breugel et al., 2015; Cardé R.T., 2015). The V glomerulus is also innervated by a GABAergic neuron that innervates all glomeruli of the antennal lobe (Lin et al., 2013), suggesting a possible mechanism for the V glomeruli's information to integrate across the entire antennal lobe, which could also contribute to general changes in awareness or behavioral activation upon exposure.

Recent studies have identified additional glomerular pathways in models that can successfully model behavior to some degree from Or-expressing ORNs alone through systematic testing (Badel et al., 2016; Bell and Wilson, 2016). Unfortunately, only 11 of the 39 odors they tested overlapped with this study, making it difficult to compare models of predictions. Additionally, it is likely that refined discrimination between odorants require inputs from the numerous pathways, a role that the species-specific *Or* pathways are suitable for. An attractive model to investigate would be if the diverse *Or* pathway offers more

flexible inputs to behavior, as is important for species-specific adaptation, or for plasticity in olfactory behavior associated with hunger and in associative learning, while the highly-conserved *Gr63a* and *Gr21a* receptor proteins act as broadly-tuned ancient pathway that codes for a default innate hedonic valence across multiple odorant classes.

STAR Methods

CONTACT FOR REAGENT AND RESOURCE SHARING

Further information and requests for resources and reagents should be directed to and will be fulfilled by the Lead Contact, Anandasankar Ray (anand.ray@ucr.edu).

EXPERIMENTAL MODEL AND SUBJECT DETAILS

Insect stocks—*Drosophila melanogaster* stocks were Canton S backcrossed to w^{1118} for 5 generations (wild-type), $Or83b^{2}$ (Larsson et al., 2004) (an *orco*− mutation) and $Gr63a^{1}$, and $Gr63a^{1}$,$Or83b^{2}$ (Jones et al., 2007; Larsson et al., 2004). *Gr63a-GAL4* (BL #9942) (Jones et al., 2007) was backcrossed to control w^{1118}. Mosquitoes used were female *Aedes aegypti* (Linnaeus 1762), Rockefeller strain.

METHOD DETAILS

***Drosophila* T-maze assays—**T-maze behavioral testing using *Drosophila* was performed as described previously (Turner and Ray, 2009), with minor modifications. Twenty males and 20 females, 3–7 days old, wet starved ~20–25 hrs were used in each trial in a T-maze without airflow, placed inside a 30 cm^3 white-walled perimeter. Odorants were of the highest available purity (Sigma-Aldrich). Chemicals were diluted in water or paraffin oil. For most odorants, tubes contained 10 ul of odorant solution or solvent, were sealed with Parafilm and allowed to volatilize for ~10 min prior to the start of each 1 min trial. For all odorants in figure 5A except ACV, chemicals were volatilized for ~3 min before start of the 1 min assay. Background levels of CO_2 in the T-maze were elevated by injecting measured volumes of 100% CO_2 into both arms to reach the indicated concentrations. Avoidance index was calculated as before (Turner and Ray, 2009). For experiments with pre-exposure, 10 ul 2,3 butanedione was added into a tube and left covered with a small ball of cotton for 30 minutes to volatilize. Test flies were introduced into the tube for a 1-minute pre-exposure and transferred to a fresh tube to rest for 2 minutes, and then loaded into the T-maze to test behaviour to spermidine (10 ul of 1%) for a 1-minute test.

$$PI = (flies in test arm - flies in control arm) / total number of flies in arms of T-maze.$$

***Drosophila* Trap assays—**For olfactory trap assays 20 *Drosophila* were released in cylindrical arenas containing 2 tube traps. Flies were transferred to a cylindrical 38.1 mm D × 84.1 mm H chamber containing a trap fashioned from an upturned 1.5 ml microcentrifuge tube with 2 mm removed from the tapered end. A pipette tip (1000 ul) was cut 2.5 cm from the narrow end and 0.5 cm from the top, and inserted into the bottom of the inverted microcentrifuge tube. Each Arena used 10 male and 10 female *Drosophila* that were starved

for ~22 hours prior to the start. Arenas were loaded at 12 PM and trials were terminated after 24 hours. Each tube trap contained 200 ul of either solvent (H_2O) or odorant dilution.

Mosquito arm-in-a-cage assay—This assay was performed as described previously (Boyle et al., 2016), with modifications. *A. aegypti* were maintained at ~27 °C and ~50% RH on a 14h: 10h L: D cycle were used. Behavioural tests were performed with 40 mated, non-blood fed, ~24 hour starved, 4–10 day old females in 30cm × 30cm × 30cm cages with a glass top to allow for video recording. The test compound solution (500μl) at the indicated concentration in water was applied evenly to a white rectangular 7cm × 6cm polyester netting (mesh size 26 × 22 holes per square inch) in a glass petri-dish. Spermidine was diluted in water. Solvent-treated and odorant-treated netting were hung in a laminar flow hood until dry. Videos were analyzed by counting the number of mosquitoes that landed on netting in snapshots occurring every 30 s for the duration of the 5 min trial. A nitrile glove (Sol-vex) was modified by adding a 5.8cm × 5cm window on the top and magnetic frames were used to secure one treated net ~1.5 mm above skin, and a second untreated net ~4.5 mm above the treated net. In this manner mosquitoes were attracted to the open window by skin emanations yet unable to contact the treated nets, or pierce the skin. Additionally the test compound did not contact the skin. Care was taken that experimenter did not use cosmetics or scented soap on their arms on the testing day. For each trial the gloved arm was inserted into the cage for 5 min and the number of landings on the test window recorded on video. Solvent controls were always tested prior to treatment.

Mosquito Two-choice skin odor assays—40 mated, non-blood fed, ~20–24 h starved, 4–14-day-old females were placed in 30 cm × 30 cm × 30 cm cages with a glass top to allow for video recording. Polyester netting (BioQuip #7250A) was cut into 15 cm × 7 cm strips. Strips were worn within socks and under shirts for ~5 hours before testing. Just prior to testing, each strip was cut into 8 squares and distributed equally between two 10 cm × 1.5 cm polystyrene petri dishes, such that each test and control dish contained 16 mesh squares. Dishes were covered with netting treated with solvent (water) or a 10% spermidine solution. 600 ul of solvent or spermidine solution was applied evenly to a 13 cm × 13 cm piece of netting in a glass Petri dish and suspended in a laminar flow hood for ~15 min to allow solvent evaporation. For each trial, control and spermidine-treated dishes were gently placed at a maximal distance apart, midway along the length of the cage. Dish position was alternated between trials, and dishes were used for no more than 4 trials. Each cage of mosquitoes was used for one trial only. Assays with < 10 landings on control plates were excluded from analysis. Videos were analyzed by counting the total number of landings on each dish throughout a 5 min trial.

Electrophysiology—Adult female and male *Drosophila* and female *A. aegypti* were tested at 3– 10, and 4–10 days, respectively, after emergence with single-sensillum extracellular recordings (SSR) as described in (Tauxe et al., 2013; Turner and Ray, 2009), with modifications. Long duration pulses of spermidine or cyclopentanone were delivered in modified 10 ml cartridges described in (Tauxe et al., 2013). For trials with inhibitors, *Drosophila* and *A. aegypti* background activity during stimulation was ~20 and ~55 spikes s^{-1}, respectively, and activation of cpA by 0.15% CO_2 was to ~90 spikes s^{-1}, unless

indicated. Spike counting for single-sensillum experiments was done manually or in combination with Igor Pro 6.2 (Wavemetrics) with the Neuromatic v2.00 macro (Jason Rothman).

QUANTIFICATION AND STATISTICAL ANALYSIS

Computational modeling of behavior—Regression analyses were conducted in R version 3.3 (R Core Team, 2016) using the step() and lm() functions. After fitting the full model, predictors were assessed in smaller subsets using an exhaustive search algorithm, applying multiple parameters for the quality of the fit. Models that reduced complexity while optimizing the R squared, Mallow's C_p and BIC statistics were cross referenced with the solution from stepwise regression, which employs an automated search for optimal predictors; the full model was fit with successive removal of predictors (backward selection) based on BIC minimization. To control for overfitting, a model including the optimal predictors was tested by applying repeated 10-fold cross-validation (1000 folds) or the bootstrap (1000 resamples), unless stated otherwise. Since the selection of predictors on training cases is not always representative, a cross-validation approach was taken to confirm and possibly identify other predictors that explained variability in PI on resamples of the odor space. Machine learning algorithms applied in support of these and other variable selection approaches were based on customized scripts in the R programing environment, along with support from the classification and regression training (caret) package (Kuhn, 2008), the kernlab (Karatzoglou et al., 2004) and e1071 (https://cran.r-project.org/web/packages/e1071/e1071.pdf) packages. Optimal predictor selection with the Boruta algorithm was similarly carried out using the implementation available in R (Kursa, et al., 2010). In cases where algorithms could be tuned, particularly for regularization, optimal values were identified by searching the space of available parameters and using the combinations that maximized predictive performance on data withheld during training.

Bootstrapping the stepwise regression addresses mild correlations amongst predictors affecting selection of an optimal model, since the choice of one predictor over another in the presence of collinearity is arbitrary and will vary with the sample profile (Miller, 2002). But in many cases the correlations are too severe and and more rigorous procedures are necessary to corroborate which predictors and models are indeed optimal. Correlated predictors (multicollinearity) can be addressed through partial least squares regression (PLS) or principal component regression (PCR), but these approaches are at the expense of detail on the best predictors. Model-specific variable importance measures are available to determine how much certain variables contribute to the best predictive equation; however, the coefficients of this model nevertheless lack interpretability. These data were ultimately excluded from the primary text. As a complement, models were also fit using regularized regression, such as ridge regression, elastic net and lasso (least absolute shrinkage and selection operator); the latter two offer alternative, built-in methods for model selection given multicollinearity by shrinking a subset of standardized predictor coefficients to zero. These regression approaches retained ab1C. But these optimal models failed to significantly improve performance beyond similarly sized OLS regression models. In the interest of thoroughness specialized predictor selection algorithms, genetic, Boruta and recursive feature elimination, were applied in conjunction with random forest regression to generate

lists of optimal predictors, without assuming a linear relationship between the preference index and responding unit.

Statistics for behavior—For all behavioral experiments with preference indexes reported, arcsine-transformed data were analyzed, and values were compared to wild type, unless indicated. Normality of the distribution was tested in each case using the Shapiro-Wilk test. Tests used are one-way ANOVA and Student's *t*-test (either using Sigma Stat or R software). One-sample *t*-tests were done by comparison to an expected mean of zero using GraphPad software available online. For all graphs, error bars indicate s.e.m. Principle component analysis and bivariate analysis were performed using JMP software package (SAS).

KEY RESOURCES TABLE

REAGENT or RESOURCE	SOURCE	IDENTIFIER
Antibodies		
Bacterial and Virus Strains		
Biological Samples		
Chemicals, Peptides, and Recombinant Proteins		
Critical Commercial Assays		

REAGENT or RESOURCE	SOURCE	IDENTIFIER
Deposited Data		
Experimental Models: Cell Lines		
Experimental Models: Organisms/Strains		
D. melanogaster: Canton-S	Bloomington Drosophila Stock Center	RRID_BDSC_64349
D. melanogaster: w^{1118}	Bloomington Drosophila Stock Center	RRID_BDSC_3605
D. melanogaster: w; TI{TI}Orco*^{2}	Bloomington Drosophila Stock Center	RRID_BDSC_23130
D. melanogaster: w; TI{TI}Gr63a*^{1}	Bloomington Drosophila Stock Center	RRID_BDSC_9941
D. melanogaster: w; Bl1/CyO; P{Gr63a-GAL4.F}35.7*	Bloomington Drosophila Stock Center	RRID_BDSC_9942
Aedes aegypti: Rockefeller strain	Laboratory of Ring Cardé, UC Riverside	Rockefeller strain
Oligonucleotides		
Recombinant DNA		
Software and Algorithms		
R version 3.3	R Development Core Team, 2016	http://www.r-project.org/

REAGENT or RESOURCE	SOURCE	IDENTIFIER
JMP software package	SAS	https://www.jmp.com/
Other		
Odorant name		**CAS number**
cis-2-hexen-1-ol		928-94-9
Cadaverine		462-94-2
Z3-Hexenol		928-96-1
1-Hexanol		111-27-3
1-Octen-3-ol		3391-86-4
Ammonium Hydroxide		1336-21-6
1-Pentanol		71-41-0
Methyloctanoate		111-11-5
Diethylsuccinate		123-25-1
6-Methyl-5-Hepten-2-0ne		110-93-0
Hexanal		66-25-1
2-Heptanone		110-43-0
Limonene		5989-27-5
Pentanoic Acid		109-52-4
Ethylpropionate		105-37-3
Hexanoic Acid		142-62-1
Linalool		78-70-6
Ethylpropionate		105-37-3
Nonanoic Acid		112-05-0
Butylacetate		123-86-4
Ethylhexanoic acid		149-57-5
Isopentanoic acid		503-74-2
Alpha-Terpineol		10482-56-1
Hexylacetate		142-92-7
3 -Methylbutanol		123-51-3
Propionic acid		79-09-4
Isobutyric acid		79-31-2
Acetic acid		64-19-7
Butyric acid		107-92-6
Octanoic acid		124-07-2
Gamma-Octalactone		104-50-7
p-Cymene		99-87-6
Beta-Myrcene		123-35-3

REAGENT or RESOURCE	SOURCE	IDENTIFIER
Eugenol		97-53-0
(1S)-(+)-3-carene		498-15-7
Geraniol		106-24-1
Pyruvic Acid		127-17-3
Geranylacetate		105-87-3
(−)-trans-Caryophyllene		87-44-5
Gamma-Decalactone		706-14-9
Phenylacetaldehyde		122-78-1
Ethyl Octanoate		106-32-1
Alpha-Humulene		6753-98-6
Delta-Decalactone		705-86-2
E3-Hexanol		623-37-0
E2-Hexenal		6728-26-3
Methylbenzoate		93-58-3
Ethylbenzoate		93-89-0
Ethyl-3-hydroxybutyrate		5405-41-4
Acetophenone		98-86-2
Gamma-hexalactone		695-06-7
Ethylbutyrate		105-54-4
Benzaldehyde		100-52-7
1-Butanol		71-36-3
Ethylhexanoate		123-66-0
Spermidine		124-20-9
Ethylenediamine		107-15-3
Piperazine		110-85-0
Butylamine		7109-73-9
Amylamine		110-58-7
Dimethylamine		124-40-3
Trimethylamine		75-50-3
1-Methyl pyrrolidine		120-94-5
Spermine		71-44-3
Cyclopentanone		120-92-3
Hexylamine		111-26-2
Ethyl pyruvate		617-35-6
Phenol		108-95-2
2,3-Butanedione		431-03-8
Geosmin		16423-19-1

Supplementary Material

Refer to Web version on PubMed Central for supplementary material.

Acknowledgments

We would like to thank Shuwie Yan for technical help, Genevieve Tauxe and Kavita Sharma for help with data analysis, Christi Scott for critical reading of the manuscript. The work was supported by a grant RO1AI087785 (NIAID) and RO1DC014092 (NIDCD) to A. Ray and R01DC013587 (NIDCD) to A. Dahanukar. The granting agencies had no role in experimental design or analysis.

References

Ai M, Min S, Grosjean Y, Leblanc C, Bell R, Benton R, Suh GSB. Acid sensing by the Drosophila olfactory system. Nature. 2010; 468:691–695. [PubMed: 21085119]

Allan SA, Bernier UR, Kline DL. Attraction of mosquitoes to volatiles associated with blood. J Vector Ecol J Soc Vector Ecol. 2006; 31:71–78.

Badel L, Ohta K, Tsuchimoto Y, Kazama H. Decoding of Context-Dependent Olfactory Behavior in Drosophila. Neuron. 2016; 91:155–167. [PubMed: 27321924]

Bell JS, Wilson RI. Behavior Reveals Selective Summation and Max Pooling among Olfactory Processing Channels. Neuron. 2016; 91:425–438. [PubMed: 27373835]

Benton R, Vannice KS, Gomez-Diaz C, Vosshall LB. Variant ionotropic glutamate receptors as chemosensory receptors in Drosophila. Cell. 2009; 136:149–162. [PubMed: 19135896]

Bernier UR, Kline DL, Barnard DR, Schreck CE, Yost RA. Analysis of human skin emanations by gas chromatography/mass spectrometry. 2. Identification of volatile compounds that are candidate attractants for the yellow fever mosquito (Aedes aegypti). Anal Chem. 2000; 72:747–756. [PubMed: 10701259]

Boyle, SM., Guda, T., Pham, CK., Tharadra, SK., Dahanukar, A., Ray, A. Natural DEET substitutes that are strong olfactory repellents of mosquitoes and flies. bioRxiv 060178. 2016. doi: http://dx.doi.org/10.1101/060178

Bräcker LB, Siju KP, Varela N, Aso Y, Zhang M, Hein I, Vasconcelos ML, Grunwald Kadow IC. Essential role of the mushroom body in context-dependent CO avoidance in Drosophila. Curr Biol CB. 2013; 23:1228–1234. [PubMed: 23770186]

Braks MAH, Takken W. Incubated human sweat but not fresh sweat attracts the malaria mosquito Anopheles gambiae SENSU STRICTO. J Chem Ecol. 1999; 25:663–672.

Braks MA, Meijerink J, Takken W. The response of the malaria mosquito, Anopheles gambiae, to two components of human sweat, ammonia and L-lactic acid, in an olfactometer. Physiol Entomol. 2001; 26:142–148.

De Bruyne M, Foster K, Carlson JR. Odor coding in the Drosophila antenna. Neuron. 2001; 30:537–552. [PubMed: 11395013]

Cardé RT. Multi-Cue Integration: How Female Mosquitoes Locate a Human Host. Curr Biol. 2015; 25:R793–795. [PubMed: 26394099]

Charlu S, Wisotsky Z, Medina A, Dahanukar A. Acid sensing by sweet and bitter taste neurons in Drosophila melanogaster. Nat Commun. 2013; 4:2042. [PubMed: 23783889]

Couto A, Alenius M, Dickson BJ. Molecular, anatomical, and functional organization of the Drosophila olfactory system. Curr Biol CB. 2005; 15:1535–1547. [PubMed: 16139208]

Croset V, Rytz R, Cummins SF, Budd A, Brawand D, Kaessmann H, Gibson TJ, Benton R. Ancient protostome origin of chemosensory ionotropic glutamate receptors and the evolution of insect taste and olfaction. PLoS Genet. 2010; 6:e1001064. [PubMed: 20808886]

Davis, Sokolove. Lactic Acid-sensitive Receptors on the Antennae of the Mosquito, Aedes aegypti. J comp Physiol. 1976; 105:43–54.

DeGennaro M, McBride CS, Seeholzer L, Nakagawa T, Dennis EJ, Goldman C, Jasinskiene N, James AA, Vosshall LB. orco mutant mosquitoes lose strong preference for humans and are not repelled by volatile DEET. Nature. 2013; 498:487–491. [PubMed: 23719379]

Dekker T, Geier M, Cardé RT. Carbon dioxide instantly sensitizes female yellow fever mosquitoes to human skin odours. J Exp Biol. 2005; 208:2963–2972. [PubMed: 16043601]

Ellin RI, Farrand RL, Oberst FW, Crouse CL, Billups NB, Koon WS, Musselman NP, Sidell FR. An apparatus for the detection and quantitation of volatile human effluents. J Chromatogr. 1974; 100:137–152. [PubMed: 4154948]

Elmore T, Ignell R, Carlson JR, Smith DP. Targeted mutation of a Drosophila odor receptor defines receptor requirement in a novel class of sensillum. J Neurosci Off J Soc Neurosci. 2003; 23:9906–9912.

Eyun SI, Young Soh H, Posavi M, Munro JB, Hughes DST, Murali SC, Qu J, Dugan S, Lee SL, Chao H, et al. Evolutionary History of Chemosensory-Related Gene Families Across the Arthropoda. Mol Biol Evol. 2017; 34(14):1838–1862. [PubMed: 28460028]

Faucher C, Forstreuter M, Hilker M, de Bruyne M. Behavioral responses of Drosophila to biogenic levels of carbon dioxide depend on life-stage, sex and olfactory context. J Exp Biol. 2006; 209:2739–2748. [PubMed: 16809465]

Faucher CP, Hilker M, de Bruyne M. Interactions of carbon dioxide and food odours in Drosophila: olfactory hedonics and sensory neuron properties. PloS One. 2013; 8:e56361. [PubMed: 23457557]

Fishilevich E, Domingos AI, Asahina K, Naef F, Vosshall LB, Louis M. Chemotaxis behavior mediated by single larval olfactory neurons in Drosophila. Curr Biol. 2005; 15:2086–2096. [PubMed: 16332533]

Gaudry Q, Hong EJ, Kain J, de Bivort BL, Wilson RI. Asymmetric neurotransmitter release enables rapid odour lateralization in Drosophila. Nature. 2013; 493:424–428. [PubMed: 23263180]

Geier M, Bosch OJ, Boeckh J. Ammonia as an attractive component of host odour for the yellow fever mosquito, Aedes aegypti. Chem Senses. 1999; 24:647–653. [PubMed: 10587497]

Ghaninia M, Hansson BS, Ignell R. The antennal lobe of the African malaria mosquito, Anopheles gambiae - innervation and three-dimensional reconstruction. Arthropod Struct Dev. 2007; 36:23–39. [PubMed: 18089085]

Van der Goes van Naters W. Inhibition among olfactory receptor neurons. Front Hum Neurosci. 2013; 7:690. [PubMed: 24167484]

Hallem EA, Ho MG, Carlson JR. The molecular basis of odor coding in the Drosophila antenna. Cell. 2004; 117:965–979. [PubMed: 15210116]

Hussain A, Zhang M, Ucpunar HK, Svensson T, Quillery E, Gompel N, Ignell R, Grunwald Kadow IC. Ionotropic Chemosensory Receptors Mediate the Taste and Smell of Polyamines. PLoS Biol. 2016; 14:e1002454. [PubMed: 27145030]

Jones WD, Cayirlioglu P, Kadow IG, Vosshall LB. Two chemosensory receptors together mediate carbon dioxide detection in Drosophila. Nature. 2007; 445:86–90. [PubMed: 17167414]

Kakkar R. Plant polyamines in flowering and fruit ripening. Phytochemistry. 1993; 33:1281–1288.

Karatzoglou A, et al. kernlab – An S4 Package for Kernel Methods in R. Journal of Statistical Software. 2004; 11(9):1–20.

Kazama H, Wilson RI. Origins of correlated activity in an olfactory circuit. Nat Neurosci. 2009; 12:1136–1144. [PubMed: 19684589]

Keene AC, Stratmann M, Keller A, Perrat PN, Vosshall LB, Waddell S. Diverse odor-conditioned memories require uniquely timed dorsal paired medial neuron output. Neuron. 2004; 44:521–533. [PubMed: 15504331]

Keller A, Vosshall LB. Influence of odorant receptor repertoire on odor perception in humans and fruit flies. Proc Natl Acad Sci U S A. 2007; 104:5614–5619. [PubMed: 17372215]

Kiss J, Korbász M, Sass-Kiss A. Study of amine composition of botrytized grape berries. J Agric Food Chem. 2006; 54:8909–8918. [PubMed: 17090141]

Knaden M, Strutz A, Ahsan J, Sachse S, Hansson BS. Spatial representation of odorant valence in an insect brain. Cell Rep. 2012; 1:392–399. [PubMed: 22832228]

Knaden M, Hansson BS. Mapping odor valence in the brain of flies and mice. Curr Opin Neurobiol. 2014; 24:34–38. [PubMed: 24492076]

Kreher SA, Mathew D, Kim J, Carlson JR. Translation of sensory input into behavioral output via an olfactory system. Neuron. 2008; 59:110–124. [PubMed: 18614033]

Krotoszynski B, Gabriel G, O'Neil H. Characterization of human expired air: a promising investigative and diagnostic technique. J Chromatogr Sci. 1977; 15:239–244. [PubMed: 893644]

Kuhn M. caret Package. Journal Of Statistical Software. 2008; 28(5):1–26. [PubMed: 27774042]

Kursa MB, Rudnicki WR. Feature Selection with the Boruta Package. Journal of Statistical Software. 2010; 36(11)

Kurtovic A, Widmer A, Dickson BJ. A single class of olfactory neurons mediates behavioural responses to a Drosophila sex pheromone. Nature. 2007; 446:542–546. [PubMed: 17392786]

Kwon HW, Lu T, Rützler M, Zwiebel LJ. Olfactory responses in a gustatory organ of the malaria vector mosquito Anopheles gambiae. Proc Natl Acad Sci U S A. 2006; 103:13526–13531. [PubMed: 16938890]

Kwon JY, Dahanukar A, Weiss LA, Carlson JR. The molecular basis of CO2 reception in Drosophila. Proc Natl Acad Sci U S A. 2007; 104:3574–3578. [PubMed: 17360684]

Larsson MC, Domingos AI, Jones WD, Chiappe ME, Amrein H, Vosshall LB. Or83b encodes a broadly expressed odorant receptor essential for Drosophila olfaction. Neuron. 2004; 43:703–714. [PubMed: 15339651]

Lin HH, Chu LA, Fu TF, Dickson BJ, Chiang AS. Parallel neural pathways mediate CO2 avoidance responses in Drosophila. Science. 2013; 340:1338–1341. [PubMed: 23766327]

Lu T, Qiu YT, Wang G, Kwon JY, Rutzler M, Kwon HW, Pitts RJ, van Loon JJA, Takken W, Carlson JR, et al. Odor coding in the maxillary palp of the malaria vector mosquito Anopheles gambiae. Curr Biol CB. 2007; 17:1533–1544. [PubMed: 17764944]

Malik AU, Singh Z. Endogenous free polyamines of mangos in relation to development and ripening. J Am Soc Hortic Sci. 2004; 129:280–286.

McDonald RE, Kushad MM. Accumulation of Putrescine during Chilling Injury of Fruits. Plant Physiol. 1986; 82:324–326. [PubMed: 16665015]

McMeniman CJ, Corfas RA, Matthews BJ, Ritchie SA, Vosshall LB. Multimodal integration of carbon dioxide and other sensory cues drives mosquito attraction to humans. Cell. 2014; 156:1060–1071. [PubMed: 24581501]

Meijerink J, Braks MA, Van Loon JJ. Olfactory receptors on the antennae of the malaria mosquito Anopheles gambiae are sensitive to ammonia and other sweat-borne components. J Insect Physiol. 2001; 47:455–464. [PubMed: 11166310]

Miller, A. Subset selection in regression. 2nd. Chapman & Hall/CRC; 2002.

Min S, Ai M, Shin SA, Suh GSB. Dedicated olfactory neurons mediating attraction behavior to ammonia and amines in Drosophila. Proc Natl Acad Sci U S A. 2013; 110:E1321–1329. [PubMed: 23509267]

Missbach C, Dweck HK, Vogel H, Vilcinskas A, Stensmyr MC, Hansson BS, Grosse-Wilde E. Evolution of insect olfactory receptors. Elife. 2014; 3:e02115. [PubMed: 24670956]

Okumu FO, Killeen GF, Ogoma S, Biswaro L, Smallegange RC, Mbeyela E, Titus E, Munk C, Ngonyani H, Takken W, et al. Development and field evaluation of a synthetic mosquito lure that is more attractive than humans. PloS One. 2010; 5:e8951. [PubMed: 20126628]

Olsen SR, Wilson RI. Lateral presynaptic inhibition mediates gain control in an olfactory circuit. Nature. 2008; 452:956–960. [PubMed: 18344978]

Ough CS, Daudt CE, Crowell EA. Identification of new volatile amines in grapes and wines. J Agric Food Chem. 1981; 29:938–941. [PubMed: 7310002]

Pan JW, McLaughlin J, Yang H, Leo C, Rambarat P, Okuwa S, Monroy-Eklund A, Clark S, Jones CD, Volkan PC. Comparative analysis of behavioral and transcriptional variation underlying CO_2 sensory neuron function and development in Drosophila. Fly (Austin). 2017; 11:239–252. [PubMed: 28644712]

Pandey S, Ranade SA, Nagar PK, Kumar N. Role of polyamines and ethylene as modulators of plant senescence. J Biosci. 2000; 25:291–299. [PubMed: 11022232]

Pham C, Ray A. Conservation of Olfactory Avoidance in Drosophila Species and Identification of Repellents for Drosophila suzukii. Sci Rep. 2015; 5:11527. [PubMed: 26098542]

Qiu YT, van Loon JJA, Takken W, Meijerink J, Smid HM. Olfactory Coding in Antennal Neurons of the Malaria Mosquito, Anopheles gambiae. Chem Senses. 2006; 31:845–863. [PubMed: 16963500]

R Development Core Team. R: A Language and Environment for Statistical Computing. R Foundation for Statistical Computing; Vienna Austria: 2016. p. 0

Robertson HM, Warr CG, Carlson JR. Molecular evolution of the insect chemoreceptor gene superfamily in Drosophila melanogaster. Proc Natl Acad Sci U S A. 2003; 100(Suppl 2):14537–14542. [PubMed: 14608037]

Root CM, Masuyama K, Green DS, Enell LE, Nassel DR, Lee CH, Wang JW. A presynaptic gain control mechanism fine-tunes olfactory behavior. Neuron. 2008; 2008(59):311–321.

Root CM, Ko KI, Jafari A, Wang JW. Presynaptic Facilitation by Neuropeptide Signaling Mediates Odor-Driven Food Search. Cell. 2011; 145:133–144. [PubMed: 21458672]

Semmelhack JL, Wang JW. Select Drosophila glomeruli mediate innate olfactory attraction and aversion. Nature. 2009; 459:218–223. [PubMed: 19396157]

Silbering AF, Rytz R, Grosjean Y, Abuin L, Ramdya P, Jefferis GSXE, Benton R. Complementary function and integrated wiring of the evolutionarily distinct Drosophila olfactory subsystems. J Neurosci Off J Soc Neurosci. 2011; 31:13357–13375.

Smallegange RC, Qiu YT, van Loon JJA, Takken W. Synergism between ammonia, lactic acid and carboxylic acids as kairomones in the host-seeking behaviour of the malaria mosquito Anopheles gambiae sensu stricto (Diptera: Culicidae). Chem Senses. 2005; 30:145–152. [PubMed: 15703334]

Stensmyr MC, Dweck HKM, Farhan A, Ibba I, Strutz A, Mukunda L, Linz J, Grabe V, Steck K, Lavista-Llanos S, et al. A conserved dedicated olfactory circuit for detecting harmful microbes in Drosophila. Cell. 2012; 151:1345–1357. [PubMed: 23217715]

Stocker RF, Lienhard MC, Borst A, Fischbach KF. Neuronal architecture of the antennal lobe in Drosophila melanogaster. Cell Tissue Res. 1990; 262:9–34. [PubMed: 2124174]

Strutz A, Soelter J, Baschwitz A, Farhan A, Grabe V, Rybak J, Knaden M, Schmuker M, Hansson BS, Sachse S. Decoding odor quality and intensity in the Drosophila brain. Elife. 2014; 3:e04147. [PubMed: 25512254]

Su CY, Menuz K, Reisert J, Carlson JR. Non-synaptic inhibition between grouped neurons in an olfactory circuit. Nature. 2012; 492:66–71. [PubMed: 23172146]

Suh GSB, Wong AM, Hergarden AC, Wang JW, Simon AF, Benzer S, Axel R, Anderson DJ. A single population of olfactory sensory neurons mediates an innate avoidance behaviour in Drosophila. Nature. 2004; 431:854–859. [PubMed: 15372051]

Suh GSB, Ben-Tabou de Leon S, Tanimoto H, Fiala A, Benzer S, Anderson DJ. Light activation of an innate olfactory avoidance response in Drosophila. Curr Biol CB. 2007; 17:905–908. [PubMed: 17493811]

Takken, W., Knols, BGJ. Olfaction in vector-host interactions. Wageningen: Wageningen Academic Publishers; 2010.

Taneja J, Guerin PM. Ammonia attracts the haematophagous bug Triatoma infestans: behavioural and neurophysiological data on nymphs. J Comp Physiol A. 1997; 181:21–34.

Tauxe GM, MacWilliam D, Boyle SM, Guda T, Ray A. Targeting a dual detector of skin and CO2 to modify mosquito host seeking. Cell. 2013; 155:1365–1379. [PubMed: 24315103]

Turner SL, Ray A. Modification of CO2 avoidance behaviour in Drosophila by inhibitory odorants. Nature. 2009; 461:277–281. [PubMed: 19710651]

Turner SL, Li N, Guda T, Githure J, Cardé RT, Ray A. Ultra-prolonged activation of CO2-sensing neurons disorients mosquitoes. Nature. 2011; 474:87–91. [PubMed: 21637258]

Valero D, Martinez D, Riquelme F. Polyamine Response to External Mechanical Bruising in Two Mandarin Cultivars. HortScience. 1998; 33:1220–1223.

van Breugel F, Riffell J, Fairhall A, Dickinson MH. Mosquitoes Use Vision to Associate Odor Plumes with Thermal Targets. Curr Biol. 2015; 25:2123–2129. [PubMed: 26190071]

van Breugel, F., Huda, A., Dickinson, MH. Drosophila have distinct activity-gated pathways that mediate attraction and aversion to CO_2. bioRxiv 227991. 2017. doi: https://doi.org/10.1101/227991

Verhulst NO, Andriessen R, Groenhagen U, Bukovinszkiné Kiss G, Schulz S, Takken W, van Loon JJA, Schraa G, Smallegange RC. Differential attraction of malaria mosquitoes to volatile blends produced by human skin bacteria. PloS One. 2010; 5:e15829. [PubMed: 21209854]

Vosshall LB, Stocker RF. Molecular architecture of smell and taste in Drosophila. Annu Rev Neurosci. 2007; 30:505–533. [PubMed: 17506643]

Wasserman S, Salomon A, Frye MA. Drosophila tracks carbon dioxide in flight. Curr Biol CB. 2013; 23:301–306. [PubMed: 23352695]

Webster B, Lacey ES, Cardé RT. Waiting with bated breath: opportunistic orientation to human odor in the malaria mosquito, Anopheles gambiae, is modulated by minute changes in carbon dioxide concentration. J of Chem Ecol. 2015; 41:59–66. [PubMed: 25572756]

Yaksi E, Wilson RI. Electrical coupling between olfactory glomeruli. Neuron. 2010; 67:1034–1047. [PubMed: 20869599]

Yao CA, Ignell R, Carlson JR. Chemosensory coding by neurons in the coeloconic sensilla of the Drosophila antenna. J Neurosci Off J Soc Neurosci. 2005; 25:8359–8367.

HIGHLIGHTS

- *Drosophila* attracted to odorants that inhibit the CO_2 avoidance neuron in a T-maze
- Attractiveness of inhibitors increases with increasing background levels of CO_2
- The CO_2-neuron and a few Ors together predict behavioral valence in a T-maze
- Inhibition is conserved in mosquitoes and impairs attraction to skin odor

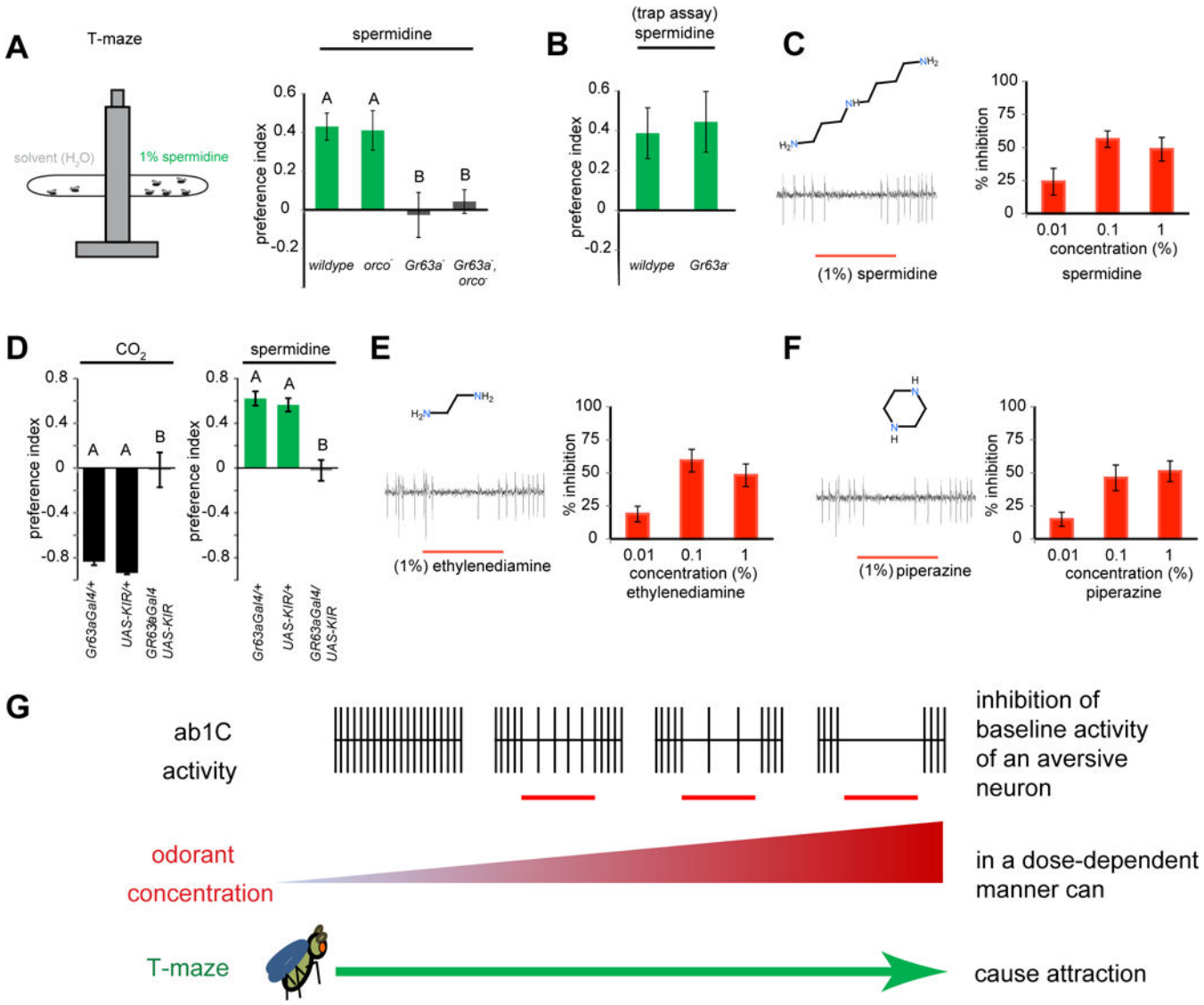

Figure 1. Polyamines cause attraction by inhibition of the CO_2-avoidance neuron in *Drosophila*

(A) Schematic of T-maze behavior assay and mean preference index for flies of indicated genotypes given a choice between solvent and 1% spermidine. (n = 8 trails per genotype, 40 flies/trial). One-way ANOVA, p <0.001. **(B)** In a trap assay, mean preference index for indicated genotypes for 1% spermidine. (n = 10 trials per genotype, 20 flies/trial). **(C)** Representative action potential trace and mean percent inhibition of ab1C activity in *orco*$^{-}$ flies during 0.5-s exposures to spermidine at indicated concentrations (n = 14). **(D)** Mean preference of flies of indicated genotypes in a T-maze for ~0.35% CO_2 and 1% spermidine (n = 8–10 per genotype). One-way ANOVA, p <0.001. **(E,F)** Representative trace and mean percent inhibition of ab1C activity in *orco*$^{-}$ flies during 0.5-s exposures to odorants at indicated concentrations (n = 14). **(G)** Model of attraction towards the source of an odorant that inhibits background firing of the aversive ab1C neuron in a dose-dependent manner. In A and D, Different letters are significantly different by Tukey's post hoc analysis. Error bars are s.e.m.

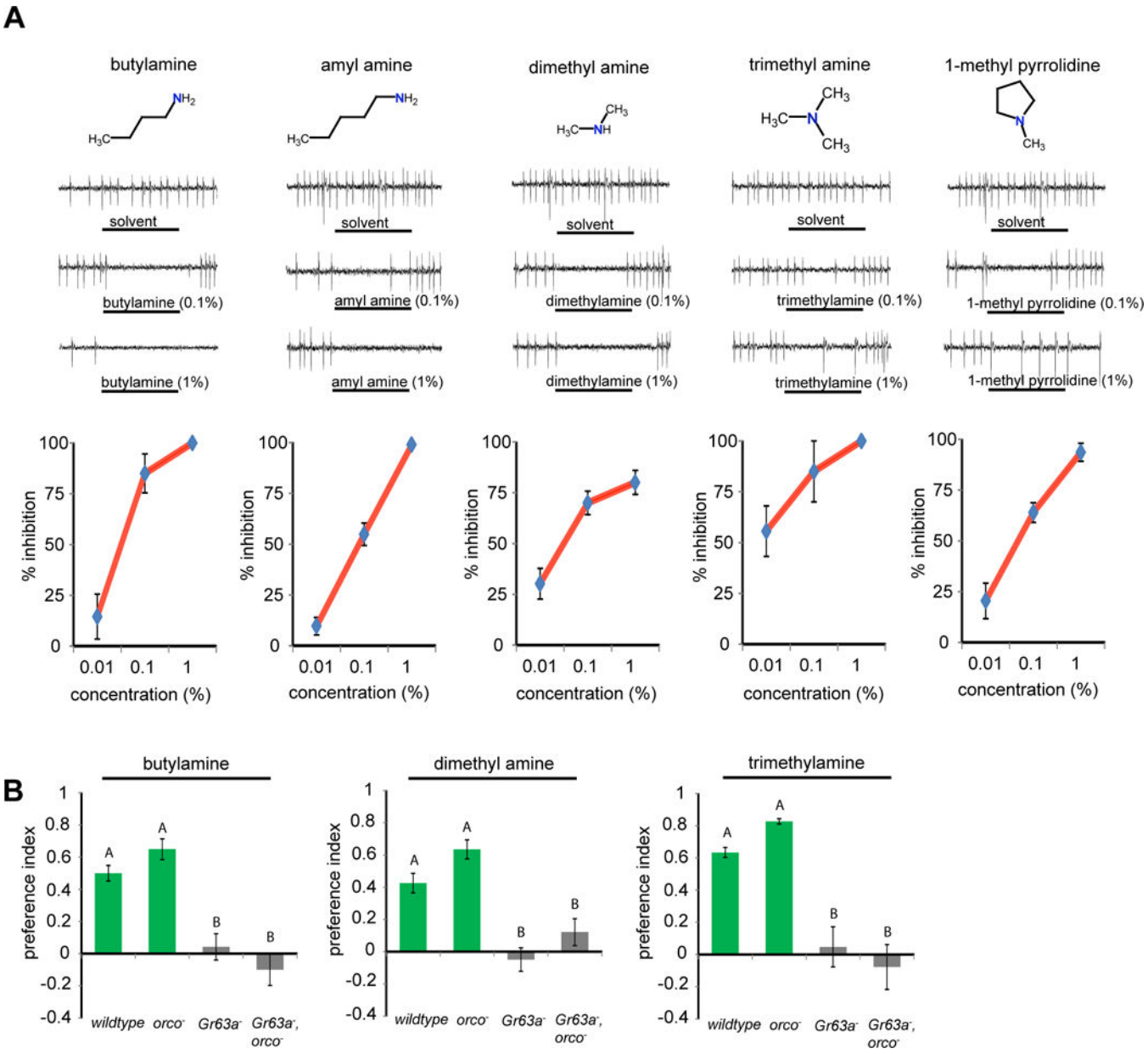

Figure 2. Amines inhibit ab1C, and *Gr63a* is necessary for attraction to amines in *Drosophila*

(A) Chemical structures, representative traces, and mean percent inhibition of ab1C activity in *orco*⁻ flies during 0.5-s exposures to the monoamines at indicated concentrations. Stimulus bar is 0.5 s (n = 14 per concentration, except for trimethyamine and butylamine, n=4). **(B)** T-maze behavior assay: mean preference index of flies of indicated genotypes to a choice between solvent and indicated odorants at 1% concentration. N = 6–16 trails per genotype (~40 flies/trial), One-way ANOVA, p <0.001 for all, genotypes marked with different letters are significantly different by Tukey's post hoc analysis. Error bars are s.e.m.

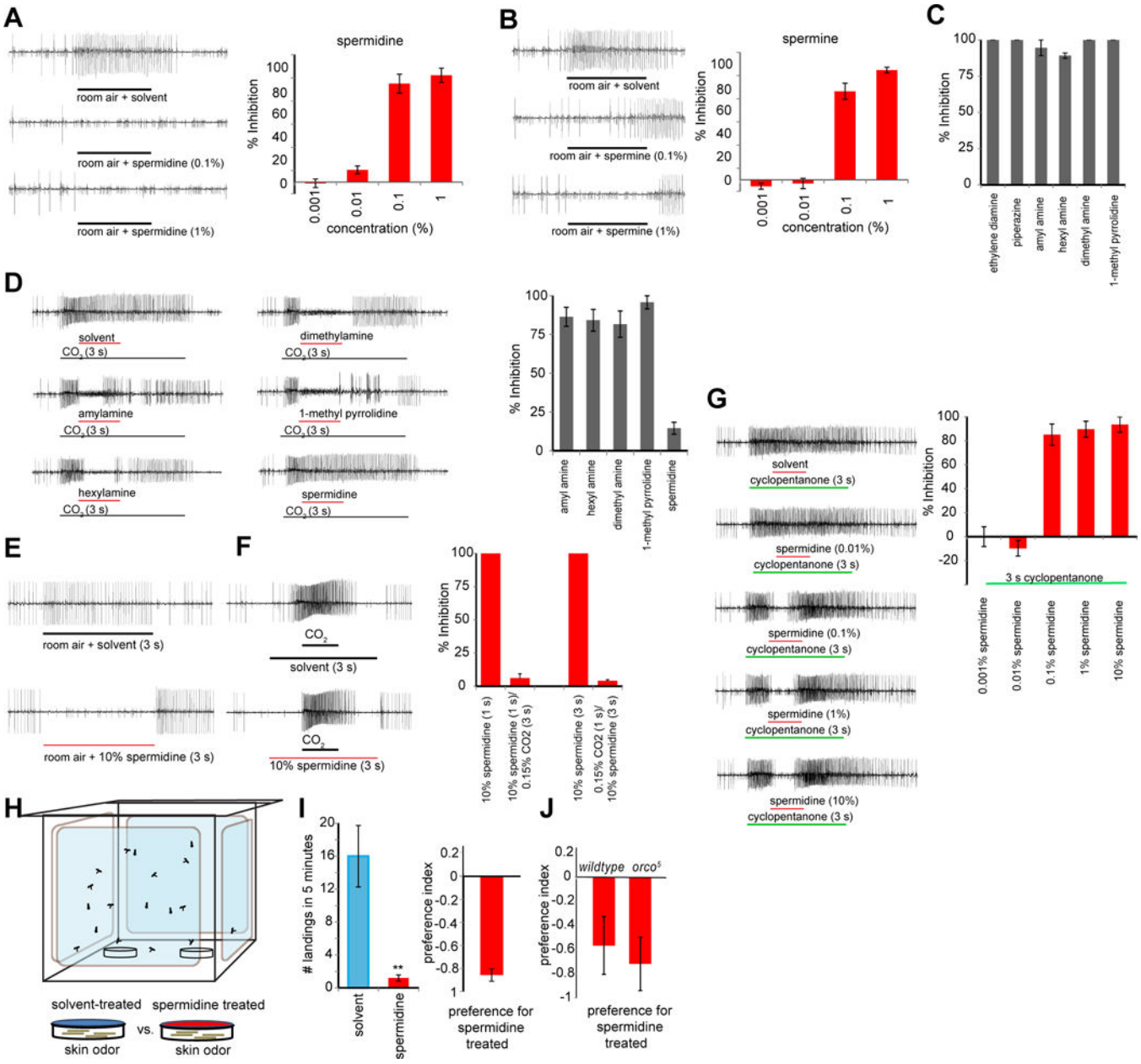

Figure 3. Amines inhibit the CO_2-receptor neuron in *Aedes aegypti*

(A, B) Representative traces and mean percent inhibition of cpA activity for **A**, spermidine (n = 6 per concentration), and **B**, spermine (n = 6 per concentration). The stimulus is room air with ambient CO_2 concentration which stimulates the ab1C neuron. **(C)** Mean percent inhibition of cpA activity by a panel of amines diluted to 1%. (n = 4 sensilla). **(D)** Representative traces and mean percent inhibition of cpA by a panel of amines (1%) when overlaid on 0.15% CO_2. (n = 5–6 sensilla). **(E)** Representative traces of a 10% spermidine pulse (3-s). (**F**) Representative traces and mean percent inhibition of cpA when a 10% spermidine pulse (1-s) is overlaid on pulse a 0.15% CO_2 (3-s), or when 0.15% CO_2 (1-s) is overlaid on 10% spermidine (3-s). (n = 4–6 sensilla). (Representative traces are shown only for trials testing CO_2 overlays onto 3-s spermidine). **(G)** Representative traces and mean

percent inhibition of cpA by indicated concentrations of spermidine when overlaid on 1% cyclopentanone (3-s). Average response to cyclopentanone alone = 79 +/− 7.6 spikes s^{-1}. (*n* = 4–6 sensilla) **(H)** Schematic of mosquito two-choice assay. **(I)** Mean number of mosquitoes landing on spermidine-treated or solvent-treated netting and preference index for a 5-min two-choice assay. (*n* = 5 trials, 40 mosquitoes/trial). *t*-test, ** $p < 0.01$, and **(J)** mean preference index in the same experimental paradigm with *A. aegypti* wild type and *orco*^{5} mutant females. (*n* = 6 trials, 40 mosquitoes/trial). Error bars are s.e.m.

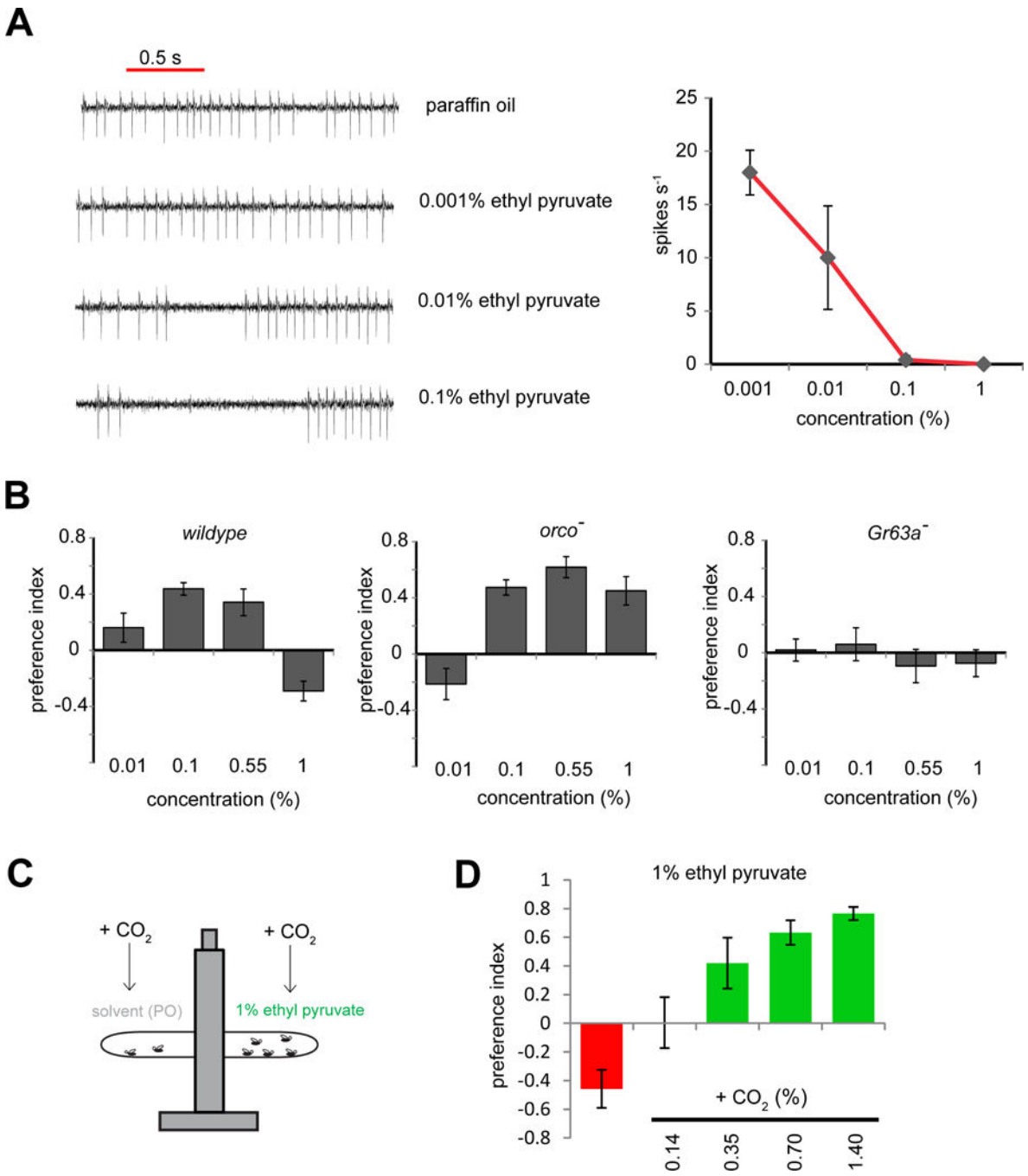

Figure 4. Attractiveness of an inhibitor is modulated by background level of CO_2

(A) Representative traces and mean activity of ab1C during 0.5 s exposures to ethyl pyruvate at indicated concentrations. (n=5 sensilla per concentration) **(B)** In a T-maze, mean preference of flies of indicated genotypes for indicated concentrations of ethyl pyruvate. (*n* = 8–10 trials per genotype, 40 flies/trial). **(B)** Schematic of T-maze assay. Prior to testing, CO_2 was injected into both arms of the T-maze to elevate background levels. **(D)** Preference in a T-maze of *wildtype* flies for 1 % ethyl pyruvate in the presence of CO_2 elevated to indicated concentrations. (*n* = 4–6 per concentration, 40 flies/trial).

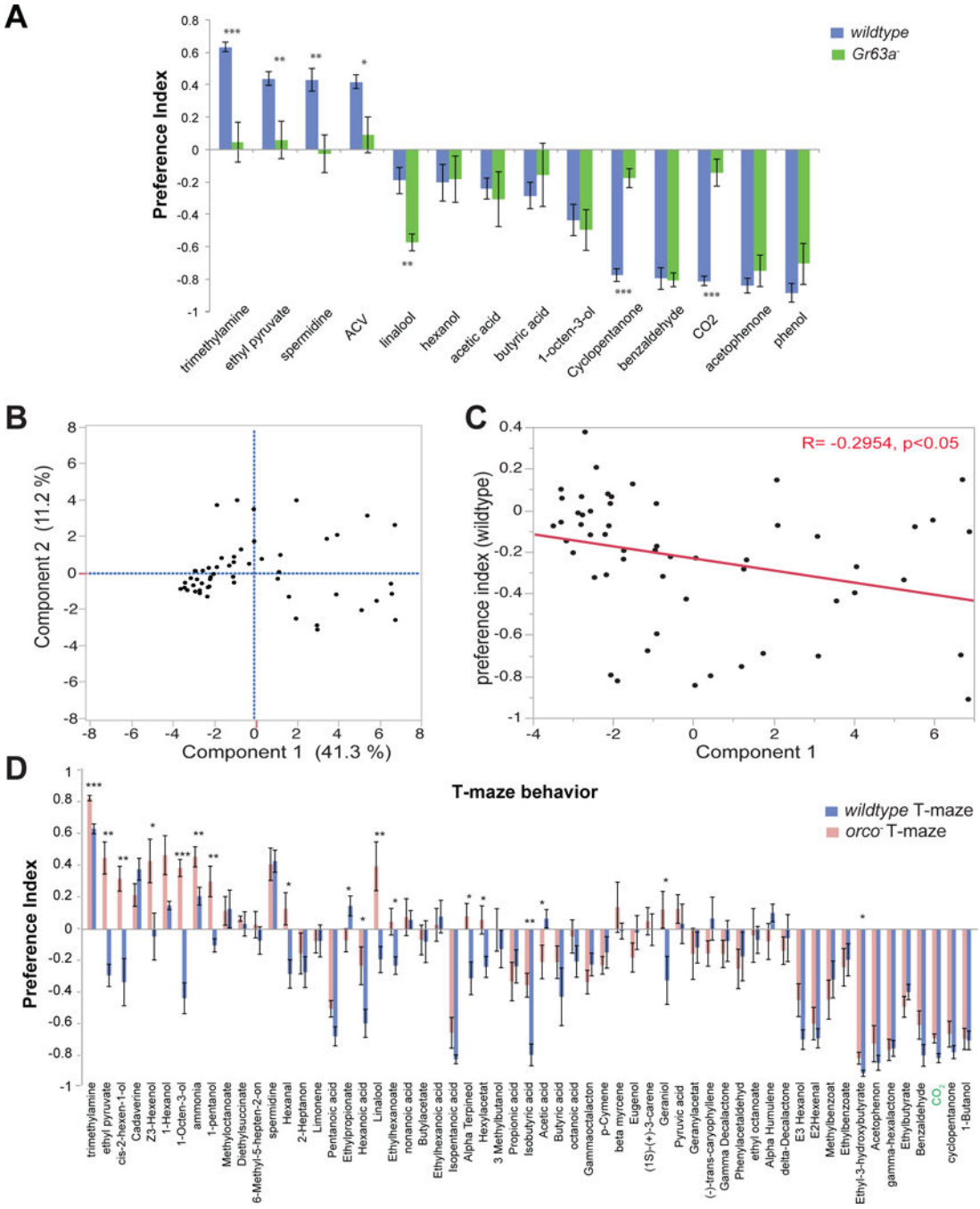

Figure 5. T-maze behavior and receptor dependency in *Drosophila*

(A) Bar graph of olfactory behavior for the indicated odorants (1% concentration) and genotypes in a T-maze: n = 6–16 trials per odorant per genotype. **(B)** Shown are the first two principle components on a 24 dimensional Odorant receptor response space for 54 odorants from Halem and Carlson, 2006. Numbers in parenthesis indicate the fraction of variance in the data represented in each axis. **(C)** Scatter plot of mean preference index from T-maze assays of each of the 54 odorants (10^{-2} dilution) vs. Principle component 1 values for each odorant. R = Pearson correlation coefficient. **(D)** Mean preference index in a T-maze

behavior assay for the indicated odorants (10^{-2} dilution) in wildtype and *orco*− *D. melanogaster* Error bars are s.e.m. *t*-test; p*<0.05, **<0.005, ***<0.001.

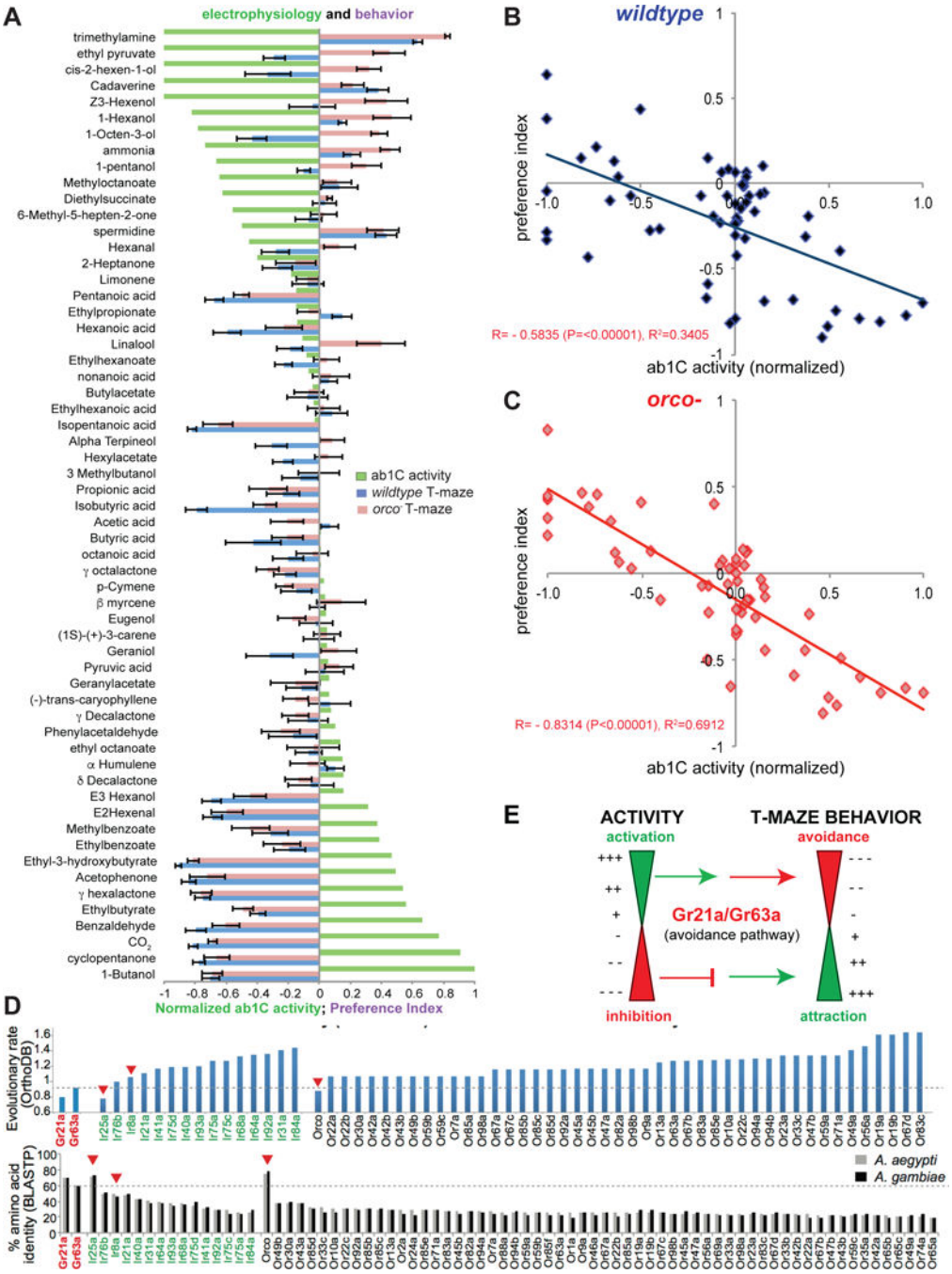

Figure 6. Broadly tuned CO_2 receptor neuron activity inversely correlates with behavior

(A) Mean ab1C electrophysiology activity to a panel of the indicated odorants (10^{-2} dilution) normalized from +1 to −1 using 1-Butanol response, and "0" as background activity. Recordings were performed in *orco*− background for ease of counting ab1C action potentials (n= 5–14). Mean ab1C electrophysiology activity is overlaid with the mean preference index of flies in a T-maze of indicated genotype (from Figure 5D). **(B,C)** Data from **(A)** shown as a scatter plots of ab1C ligand activity vs. mean preference index in T-maze behavior for *D. melanogaster* that are wild-type (B), and *orco*− mutant (C). Pearson's

correlation coefficient (R) is indicated for each plot showing significant correlation. **(D** The evolutionary rate (top) of receptors obtained from OrthoDB from Dipteran inclusive orthologs. All receptors from the Or, Ir and Gr family that are known to play a role in olfaction or expressed in the olfactory system are included that appear in the Dipteran inclusive ortholog search. Red arrowheads indicate known co-receptors. (Bottom) Percentage amino acid identity of the top BLASTP hit for the indicated *D. melanogaster* receptor in the two indicated mosquito genomes. **(F)** Model: In *Drosophila melanogaster* activation in a dose-dependent manner of the CO_2 receptor neuron leads to avoidance, and inhibition in a dose-dependent manner leads to attraction.

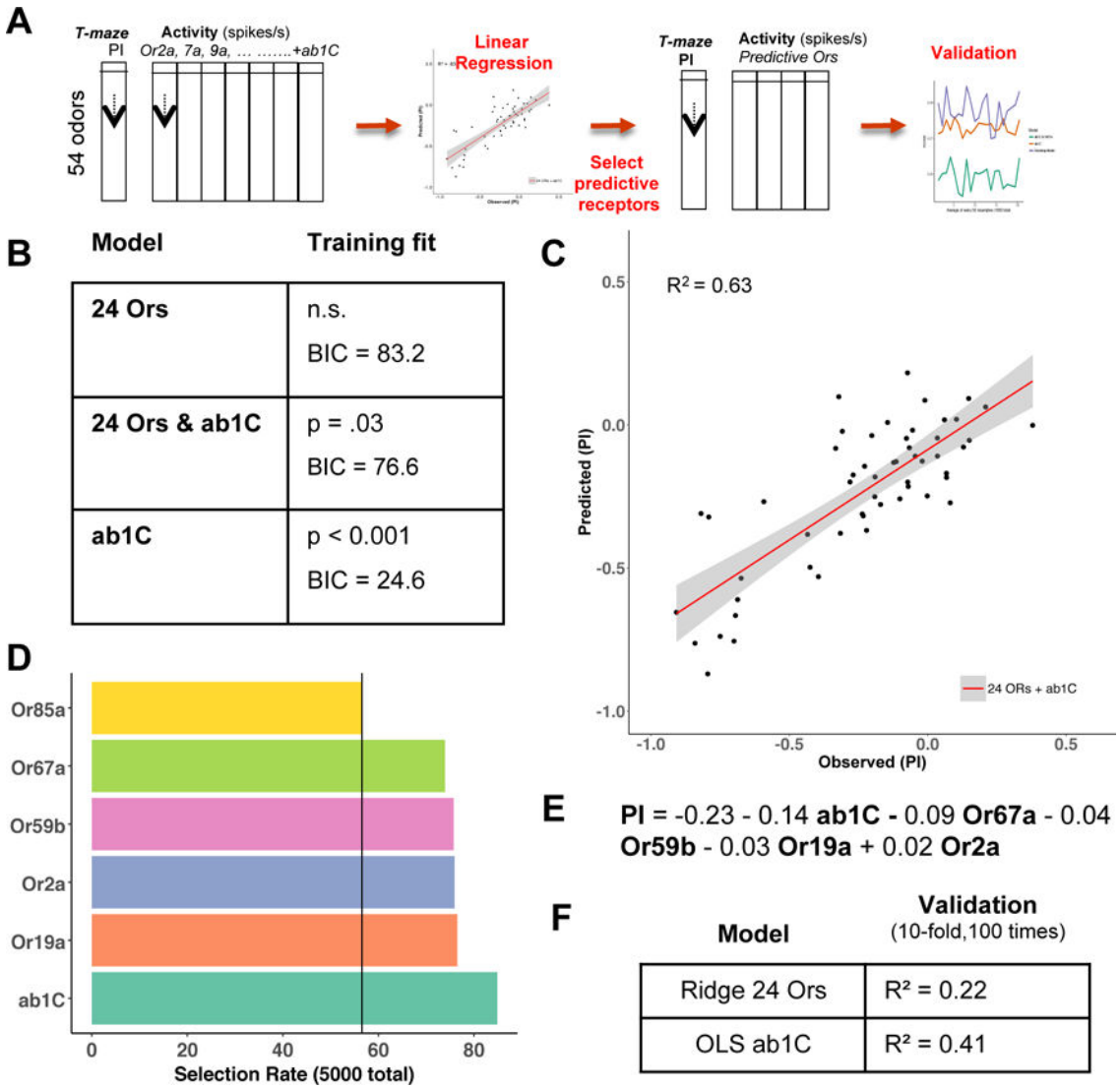

Figure 7. CO_2 receptor neuron activity is required for prediction of odor valence

A) Sample workflow of the modeling approach. The T-maze preference index for 54 odor × 24 Or-response matrix was used to predict the PI; this Or-only model was initially fit using OLS regression and was then retested for fit after adding ab1C activity for the 54 odorants. Uninformative predictors were removed and the reduced model was validated. **B)** Tabulated measures of fit are shown for the labeled model on the original data. **C)** Predicted PI was plotted as a function of the observed PI for the 24OR+ ab1C model; the red line depicts the linear trend while the overlaying gray band is the standard error for the fit. **D)** Predictors that are selected most frequently and their selection rates, across 5000 iterations of stepwise regression, resampling the 54-odorant set on each run. The black vertical line is the empirically determined threshold for consistent selection out of 5000 iterations. **E)** Linear equation of the optimal predictors. Units for the coefficients reflect the Z transformed spikes/s. **F)** Average performance on 1000 cross-validation test folds is shown for two

models. To ensure optimal performance and stability of the larger Or-only model, the test average is shown for ridge regression and compared to ab1C alone using OLS regression.